

---

# Provable Subspace Identification of Nonlinear Multi-view CCA

---

Zhiwei Han

Steffan Matthes

Hao Shen

fortiss GmbH, Munich, Germany  
Technical university of Munich  
{han,matthes,shen}@fortiss.org

## Abstract

We investigate the identifiability of nonlinear Canonical Correlation Analysis (CCA) in a multi-view setup, where each view is generated by an unknown nonlinear map applied to a linear mixture of shared latents and view-private noise. Rather than attempting exact unmixing, a problem proven to be ill-posed, we instead reframe multi-view CCA as a basis-invariant subspace identification problem. We prove that, under suitable latent priors and spectral separation conditions, multi-view CCA recovers the pairwise correlated signal subspaces up to view-wise orthogonal ambiguity. For  $N \geq 3$  views, the objective provably isolates the jointly correlated subspaces shared across all views while eliminating view-private variations. We further establish finite-sample consistency guarantees by translating the concentration of empirical cross-covariances into explicit subspace error bounds via spectral perturbation theory. Experiments on synthetic and rendered image datasets validate our theoretical findings and confirm the necessity of the assumed conditions.

## 1 Introduction

Paired multi-view data are ubiquitous, arising from multimodal sensing, multi-camera systems, and synchronized instruments. A primary objective of representation learning is to disentangle latent structures shared across views while discarding view-private variation from *nonlinear* observations, yielding representations that are interpretable, robust to nuisance perturbations, and transferable across modalities. Correlation-based methods, most notably canonical correlation analysis (CCA) and its multi-view generalizations [Kettenring, 1971], address this objective

by learning whitened representations that are maximally aligned in second-order statistics. Such methods and their whitening-based variants are also widely used in self-supervised learning to prevent feature collapse and stabilize training [Zbontar et al., 2021, Weng et al., 2022, Ermolov et al., 2021, He and Ozay, 2022, Kalapos and Gyires-Tóth, 2024].

Despite their empirical success, what nonlinear CCA *identifies* under realistic nonlinear distortions remains insufficiently characterized. Given the impossibility of unsupervised source recovery from general nonlinear mixtures [Hyvärinen and Pajunen, 1999, Locatello et al., 2019], multi-view constraints have emerged as a prominent structural prior to restore identifiability. Existing CCA-based guarantees either impose post-nonlinear assumptions [Lyu and Fu, 2020] or establish equivalence up to arbitrary invertible transforms [Lyu et al., 2021]. While recent work establishes affine identifiability under general nonlinear mixing in the general two-view regime [Han et al., 2025], what additional views enable in a basis-invariant sense remains unclear.

In this work, we address this question through the lens of *subspace identification*. We study an additive multi-view generative process where each view is produced by an unknown smooth invertible map applied to a view-specific source. Each source decomposes into a linearly mixed shared latent vector plus view-private noise, relaxing coordinate-wise independence as in ICA and aligning with content–style methodology in causal representation learning [Von Kügelgen et al., 2021, Yao et al., 2024b]. Because the mixing matrices are not identifiable, we target their basis-invariant *signal subspaces* instead. We show that multi-view CCA acts as an *intersection filter* over latent factors: it isolates the jointly correlated structure shared across views while eliminating view-private variations, and we also provide finite-sample guarantees for the empirical estimator.

We summarize our contributions as follows:

- We propose an  $N$ -view additive latent model that relaxes component-wise independence assumption and casts nonlinear CCA as a basis-invariant subspace identification problem.
- We prove that generalized nonlinear CCA ( $N \geq 3$ ) isolates the jointly correlated signal subspaces, formalizing the objective as an intersection filter over latent factors.
- We establish finite-sample consistency for empirical multi-view CCA, translating concentration of second-order statistics into explicit subspace recovery rates via spectral perturbation bounds.
- We validate the theory on synthetic and rendered image datasets, corroborating correlated-subspace recovery and the necessity of the stated conditions.

## 2 Related Work

**Identifiable Disentanglement and Nonlinear ICA.** Identifiable representation learning seeks latent structure recovery up to unavoidable symmetries, rooted in blind source separation and independent component analysis (ICA) [Barlow et al., 1989, Comon, 1994, Cardoso, 1998]. Without inductive biases, exact recovery from i.i.d. observations under general nonlinear mixing is fundamentally impossible [Hyvärinen and Pajunen, 1999, Locatello et al., 2019]. To restore identifiability, prior works introduce symmetry-breaking priors, such as temporal dynamics, nonstationarity, auxiliary variables, interventions, or multi-view constraints [Hyvarinen and Morioka, 2016, 2017, Hyvarinen et al., 2019, Khemakhem et al., 2020, Locatello et al., 2020, Shu et al., 2019].

**Identifiability from Multiple Views.** Multi-view observations provide cross-view constraints that mitigate the non-identifiability of single-view mixing. In linear regimes, exploiting higher-order moments or multi-view ICA isolates shared and view-specific sources up to standard permutation and scaling ambiguities [Podosinnikova et al., 2016, Pandeva and Forré, 2023]. For nonlinear mixtures, contrastive objectives can identify shared factors up to component-wise invertible transformations under independent-source and structured noise assumptions [Zimmermann et al., 2021, Gresele et al., 2020, Matthes et al., 2023, Gálvez et al., 2023]. Recent advances relax the independent-source assumption by exploiting causal latent structures, shifting the target to *block-identifiability*. These methods are increasingly unified under partial-observability frameworks, which derive identifiability from underlying graphical structures under mild conditions [Von Kügelgen et al., 2021, Schölkopf et al., 2016, Sturma et al., 2023, Yao et al., 2024b,a, Ahuja et al., 2022, Daunhawer et al., 2023b,

Xu et al., 2024, Locatello et al., 2020].

### Identifiability of Nonlinear Multi-view CCA.

CCA aligns views using second-order statistics post-whitening. While classical results establish the uniqueness of linear CCA under Lancaster distribution families [Lancaster, 1958, Eagleson, 1964], guarantees for nonlinear CCA remain limited. Existing results either rely on restrictive post-nonlinear assumptions [Lyu and Fu, 2020] or weaken the recovery guarantee to arbitrary invertible transformations under general mixing [Lyu et al., 2021]. Recent work establishes affine identifiability for nonlinear CCA in the general two-view regime [Han et al., 2025], but does not characterize, in a basis-invariant manner, what additional views identify. In contrast, we shift the target from mixing recovery to signal subspace identification and show that, under suitable latent priors, generalized multi-view CCA isolates the jointly correlated subspaces shared across views.

## 3 Problem Formulation

**Multi-view Generative Process.** We observe i.i.d. samples from  $N$  views, denoted by  $\{\mathbf{x}_i\}_{i=1}^N$ . For each view  $i \in [N] := \{1, \dots, N\}$ , the observation  $\mathbf{x}_i \in \mathcal{X}_i \subseteq \mathbb{R}^{d_{x_i}}$  is generated from an *unobserved* view-specific latent source  $\mathbf{s}_i \in \mathcal{S}_i \subseteq \mathbb{R}^{d_{s_i}}$  via an *unknown, generally nonlinear* generating function  $\mathbf{g}_i : \mathcal{S}_i \rightarrow \mathcal{X}_i$ , i.e.,  $\mathbf{x}_i = \mathbf{g}_i(\mathbf{s}_i)$ . Here,  $\mathcal{S}_i$  and  $\mathcal{X}_i$  denote the source and observation spaces of view  $i$ , respectively, and  $d_{(\cdot)}$  is the dimension of the underlying ambient space.

Formally, we define the multi-view generative process via an additive-noise latent construction at the source level as follows: for each  $i \in [N]$ , we have

$$\mathbf{x}_i = \mathbf{g}_i(\mathbf{s}_i), \quad \mathbf{s}_i = \mathbf{A}_i \mathbf{c} + \boldsymbol{\epsilon}_i, \quad \mathbf{c} \sim p_{\mathbf{c}}, \quad \boldsymbol{\epsilon}_i \sim p_{\boldsymbol{\epsilon}_i}, \quad (1)$$

where  $\mathbf{c} \in \mathbb{R}^{d_c}$  is a latent vector shared across views,  $\boldsymbol{\epsilon}_i \in \mathbb{R}^{d_{s_i}}$  captures view-private variation, and  $\mathbf{A}_i \in \mathbb{R}^{d_{s_i} \times d_c}$  is a view-specific mixing matrix, e.g., arising from a linear structural causal model.

Our generative process generalizes the single-view model of Lyu and Fu [2022] to  $N$  views, with view-dependent mixing matrices  $\{\mathbf{A}_i\}_{i=1}^N$  and nonlinear maps  $\{\mathbf{g}_i\}_{i=1}^N$ . Unlike standard ICA assumptions that enforce coordinate-wise independence [Hyvarinen and Morioka, 2016, 2017, Hyvarinen et al., 2019, Khemakhem et al., 2020], the shared component mixture  $\mathbf{A}_i \mathbf{c}$  induces structured dependencies within each source  $\mathbf{s}_i$ , e.g., as in causal latent models, consistent with the checkerboard-type dependencies of Matthes et al. [2023]. Interpreting  $\mathbf{c}$  and  $\boldsymbol{\epsilon}_i$  as shared *content* and view-private *style*, our model differs from concatenation-based multi-view formulations in causal

representation learning [Daunhawer et al., 2023a, Yao et al., 2024b]. Moreover, it connects to partial observability [Yao et al., 2024b]: if  $\mathbf{A}_i$  is rank-deficient, then components of  $\mathbf{c}$  in  $\text{null}(\mathbf{A}_i)$  are unobservable in view  $i$ .

**Latent Structure.** Although additive noise models are prevalent in factor identifiability [Park, 2020, Matthes et al., 2023] and causal inference [Peters et al., 2011, Mooij et al., 2011, Hoyer et al., 2008], their implications for *subspace identification* have not been systematically characterized for subspace identification. Since CCA aggregates pairwise objectives, our analysis centers on the cross-view joint distribution of any source pair  $(\mathbf{s}_i, \mathbf{s}_j)$  over  $\mathcal{S}_i \times \mathcal{S}_j$  with  $d_{\mathcal{S}_i}, d_{\mathcal{S}_j} \geq 2$  induced by this additive structure.

**Assumption 1** (Latent Distributional Prior). For each  $i \in [N]$ , let  $\mathbf{c} \in \mathbb{R}^{d_c}$  and  $\boldsymbol{\epsilon}_i \in \mathbb{R}^{d_{\mathcal{S}_i}}$  denote the shared and private latent vectors as in Equation 1.

**1. Latent Factorization.** The shared latent  $\mathbf{c}$  and the private latents  $\{\boldsymbol{\epsilon}_i\}_{i=1}^N$  are mutually independent, and the coordinates of each vector are i.i.d.

$$p_{\mathbf{c}}(\mathbf{c}) = \prod_{j=1}^{d_c} p_{\phi}(c_j), \quad p_{\boldsymbol{\epsilon}_i}(\boldsymbol{\epsilon}_i) = \prod_{j=1}^{d_{\mathcal{S}_i}} p_{\phi}(\epsilon_{ij}),$$

$$p(\mathbf{c}, \boldsymbol{\epsilon}_1, \dots, \boldsymbol{\epsilon}_N) = p_{\mathbf{c}}(\mathbf{c}) \prod_{i=1}^N p_{\boldsymbol{\epsilon}_i}(\boldsymbol{\epsilon}_i).$$

**2. Second-moment Isotropy.** The shared latent vector  $\mathbf{c}$  and private latent vectors  $\{\boldsymbol{\epsilon}_i\}_{i=1}^N$  are isotropic with identity covariance. For all  $i \in [N]$ :

$$\mathbb{E}[\mathbf{c}] = \mathbf{0}, \quad \text{Cov}(\mathbf{c}) = \mathbf{I}_{d_c}, \quad \mathbb{E}[\boldsymbol{\epsilon}_i] = \mathbf{0}, \quad \text{Cov}(\boldsymbol{\epsilon}_i) = \mathbf{I}_{d_{\mathcal{S}_i}}.$$

Moreover, the univariate marginals ( $p_{\phi}$ ) belong to distribution families admitting a bivariate polynomial expansion (Theorem 4.1 of Eagleson [1964]), including Gaussian, Gamma, negative binomial, Poisson, and hypergeometric distributions.

We present our identifiability theory under the Gaussian prior for practical relevance and notational convenience, and show in the supplementary material how other admissible priors are compatible with our framework.

**Learning Objective.** We emphasize that the exact mixing matrices  $\mathbf{A}_i$  are fundamentally unidentifiable. Instead, we target their basis-invariant shared signal subspaces. Specifically, we aim to learn view-specific encoders  $\mathbf{f}_i : \mathcal{X}_i \rightarrow \mathcal{Z} \subseteq \mathbb{R}^{d_{\mathcal{Z}}}$  that remove the nonlinear distortions from  $\mathbf{g}_i$  and recover the shared signal subspaces under appropriate structural priors. For simplicity and practical convenience, we use a shared representation dimension  $d_{\mathcal{Z}}$  across views.

**Notations.** Throughout, scalars are denoted by plain letters. Random vectors and vector valued functions are denoted by bold lowercase letters. Matrices are denoted by bold uppercase letters. Sets and spaces are denoted by calligraphic letters.

## 4 Preliminaries

### 4.1 Nonlinear Multi-view CCA

CCA learns encoders whose whitened representations maximize cross-view correlation measured by singular values of normalized cross-covariances.

#### Generalized CCA for Multi-view Learning.

Under the multi-view generative process in Equation 1, generalized CCA [Kettenring, 1971] aggregates pairwise objectives across all view pairs as

$$J := \sum_{1 \leq i < j \leq N} \left\| \boldsymbol{\Sigma}_{ii}^{-1/2} \boldsymbol{\Sigma}_{ij} \boldsymbol{\Sigma}_{jj}^{-1/2} \right\|_*, \quad (2)$$

where  $\|\cdot\|_*$  is the nuclear norm,  $\boldsymbol{\Sigma}_{ii} := \text{Cov}(\mathbf{f}_i(\mathbf{x}_i)) \succ 0$  and  $\boldsymbol{\Sigma}_{jj} := \text{Cov}(\mathbf{f}_j(\mathbf{x}_j)) \succ 0$ , while  $\boldsymbol{\Sigma}_{ij} := \text{Cov}(\mathbf{f}_i(\mathbf{x}_i), \mathbf{f}_j(\mathbf{x}_j))$  denotes the cross-covariance matrix between  $\mathbf{f}_i$  and  $\mathbf{f}_j$ .

**CCA in the source domain.** Let the induced representation mapping for view  $i \in [N]$  be  $\mathbf{h}_i := \mathbf{f}_i \circ \mathbf{g}_i : \mathcal{S}_i \rightarrow \mathcal{Z}$ . By reparameterization invariance (Lemma 6; [Han et al., 2025]), for all  $1 \leq i < j \leq N$ ,  $\text{Cov}(\mathbf{f}_i(\mathbf{x}_i), \mathbf{f}_j(\mathbf{x}_j)) = \text{Cov}(\mathbf{h}_i(\mathbf{s}_i), \mathbf{h}_j(\mathbf{s}_j))$  and  $\text{Cov}(\mathbf{f}_i(\mathbf{x}_i)) = \text{Cov}(\mathbf{h}_i(\mathbf{s}_i))$ . Consequently, optimizing Equation 2 over  $\{\mathbf{f}_i\}$  is mathematically equivalent to optimizing it over the induced representation mapping  $\mathbf{h}_i$ . This property establishes a bijection between population maximizers in the representation and source spaces, allowing us to reduce our identifiability analysis directly from  $\{\mathbf{f}_i\}_{i=1}^N$  to the mappings  $\{\mathbf{h}_i\}_{i=1}^N$ .

### 4.2 Whitening and Canonicalization

The full-rank condition enforced by whitening [Weng et al., 2022], or its relaxation such as soft-whitening [Zbontar et al., 2021], is essential for ensuring a well-posed CCA objective and preventing representation collapse [Ermolov et al., 2021]. Both properties are critical to our identifiability analysis.

**Whitened Representations.** For each view  $i \in [N]$ , let  $\boldsymbol{\mu}'_i := \mathbb{E}[\mathbf{h}_i(\mathbf{s}_i)]$  and  $\boldsymbol{\Sigma}'_{ii} := \text{Cov}(\mathbf{h}_i(\mathbf{s}_i)) \succ 0$ . A whitening matrix  $\mathbf{W}_i \in \mathbb{R}^{d_{\mathcal{Z}} \times d_{\mathcal{Z}}}$  satisfies  $\mathbf{W}_i \boldsymbol{\Sigma}'_{ii} \mathbf{W}_i^{\top} = \mathbf{I}$ , defining the whitened representation mapping:

$$\tilde{\mathbf{h}}_i(\mathbf{s}_i) := \mathbf{W}_i(\mathbf{h}_i(\mathbf{s}_i) - \boldsymbol{\mu}'_i), \quad \text{Cov}(\tilde{\mathbf{h}}_i(\mathbf{s}_i)) = \mathbf{I}. \quad (3)$$

The canonical choice is the symmetric inverse square root,  $\mathbf{W}_i = \boldsymbol{\Sigma}'_{ii}{}^{-\frac{1}{2}}$ . While orthogonal left-multiplication of  $\mathbf{W}_i$  defines the equivalence class for our identifiability theorem, the CCA objective remains strictly invariant to this ambiguity since it depends solely on the orthogonally invariant singular values of  $\tilde{\boldsymbol{\Sigma}}_{ij}$ .

**Canonicalization via Whitening.** whitening-induced canonicalization removes scale and within-view linear ambiguities, reducing the feasible set of representations to orthonormal directions in  $L^2$ . Fix a view  $i \in [N]$  and consider the whitened representation mapping  $\tilde{\mathbf{h}}_i(\mathbf{s}_i)$ . Let  $\{\xi_{i,n}\}_{n \geq 1}$  denote a fixed orthonormal basis of the function space of  $\tilde{\mathbf{h}}$ . Each component of  $\tilde{\mathbf{h}}_i$  admits the following orthonormal basis expansion: for the component  $j \in [d_{\mathbf{Z}}]$ ,

$$\tilde{h}_{i,j}(\mathbf{s}_i) = \sum_{n \geq 1} \alpha_{i,j,n} \xi_{i,n}(\mathbf{s}_i), \quad \alpha_{i,j,n} := \langle \tilde{h}_{i,j}, \xi_{i,n} \rangle_{L^2(\mu_i)},$$

where  $\boldsymbol{\alpha}_{i,r} = [\alpha_{i,j,1}, \dots, \alpha_{i,j,\infty}]$  denotes the corresponding coefficient vector under the basis  $\{\xi_{i,n}\}_{n \geq 1}$ . The whitening constraint is equivalent to the orthonormality of these coefficient vectors across components within the same view  $i$ :

$$\boldsymbol{\alpha}_{i,p}^\top \boldsymbol{\alpha}_{i,q} = \delta_{pq}, \quad p, q \in [d_{\mathbf{Z}}], \quad (4)$$

where  $\delta_{pq}$  is the Kronecker-delta function, i.e.,  $\delta_{pq} = 1$  iff  $p = q$  and 0 otherwise. Whitening canonically enforces (i) decorrelation between representation components and (ii) unit normalization of each component in function space. Equivalently, the coefficient matrix  $\mathbf{A}_i$  with rows  $\boldsymbol{\alpha}_{i,r}^\top$  satisfies  $\mathbf{A}_i \mathbf{A}_i^\top = \mathbf{I}$ .

## 5 Theory

### 5.1 Orthogonal Polynomial Expansion of the Canonical Density

In this subsection, we characterize the spectral structure underlying the pairwise joint density between view-specific sources, induced by the additive multi-view latent model in Equation 1. Specifically, we show that a whitening transformation induces a *canonical coordinate system* in which the pairwise joint density factorizes into independent bivariate distributions parameterized by their canonical correlations.

**Canonical Coordinate System.** Under the mutual independence and i.i.d. conditions in Assumption 1.1, let

$$\mathbf{W}_i := \text{Cov}(\mathbf{s}_i)^{-\frac{1}{2}} = (\mathbf{A}_i \mathbf{A}_i^\top + \mathbf{I})^{-\frac{1}{2}}, \quad i \in [N]$$

be a whitening matrix for the view-specific source  $\mathbf{s}_i$ . For any pair of views  $1 \leq i < j \leq N$ , the dependency structure of the view-specific sources  $(\mathbf{s}_i, \mathbf{s}_j)$  is captured by their normalized cross-covariance matrix:

$$\mathbf{R}_{ij} := \text{Cov}(\mathbf{W}_i \mathbf{s}_i, \mathbf{W}_j \mathbf{s}_j) = \mathbf{W}_i \mathbf{A}_i \mathbf{A}_j^\top \mathbf{W}_j^\top. \quad (5)$$

We consider the following singular value decomposition,

$$\mathbf{R}_{ij} = \mathbf{U}_{ij} \mathbf{T}_{ij} \mathbf{V}_{ij}^\top, \quad \mathbf{U}_{ij} \in O(d_{\mathcal{S}_i}), \quad \mathbf{V}_{ij} \in O(d_{\mathcal{S}_j})$$

where  $\mathbf{T}_{ij} \in \mathbb{R}^{d_{\mathcal{S}_i} \times d_{\mathcal{S}_j}}$  is a rectangular diagonal matrix containing the singular values  $1 > t_{ij,1} \geq \dots \geq t_{ij,r_{ij}} \geq 0$  on its main diagonal, and let  $r_{ij} := \text{rank}(\mathbf{A}_i \mathbf{A}_j^\top)$ .

**Lemma 1** (Canonical Factorization). *Under the isotropic Gaussian prior in Assumption 1.2, define the canonical coordinates and denote  $(\mathbf{U}_{ij}, \mathbf{V}_{ij})$  as the corresponding canonicalizers,*

$$\mathbf{u} = \mathbf{U}_{ij}^\top \mathbf{W}_i \mathbf{s}_i, \quad \mathbf{v} = \mathbf{V}_{ij}^\top \mathbf{W}_j \mathbf{s}_j. \quad (6)$$

By the change-of-variables formula, the induced joint density is

$$p_{\mathbf{u},\mathbf{v}}(\mathbf{u}, \mathbf{v}) = p_{\mathbf{s}_i, \mathbf{s}_j}(\mathbf{W}_i^{-1} \mathbf{U}_{ij} \mathbf{u}, \mathbf{W}_j^{-1} \mathbf{V}_{ij} \mathbf{v}) \cdot |\det \mathbf{W}_i|^{-1} |\det \mathbf{W}_j|^{-1}.$$

Moreover,  $p_{\mathbf{u},\mathbf{v}}$  factorizes as

$$p_{\mathbf{u},\mathbf{v}}(\mathbf{u}, \mathbf{v}) = \underbrace{\prod_{k=1}^{r_{ij}} \phi_{t_{ij,k}}(u_k, v_k)}_{\mathcal{K}_{ij}(\mathbf{u}[1:r_{ij}], \mathbf{v}[1:r_{ij}])} \prod_{m=r_{ij}+1}^{d_{\mathcal{S}_i}} \phi(u_m) \prod_{n=r_{ij}+1}^{d_{\mathcal{S}_j}} \phi(v_n),$$

where  $\phi$  is the standard normal density and  $\phi_t$  is the standardized bivariate normal density with correlation  $t$ .

*Remark 1* (Information-Theoretic Interpretation). The factorization in Lemma 1 implies that the cross-view interaction decouples into  $r_{ij}$  independent Gaussian coordinates:

$$v_k = t_{ij,k} u_k + \sqrt{1 - t_{ij,k}^2} \varepsilon_k, \quad \varepsilon_k \sim \mathcal{N}(0, 1).$$

where the canonical correlation  $t_{ij,k}$  directly governs the effective *signal-to-noise ratio* (SNR)  $\rho_{ij,k} := t_{ij,k}^2 / (1 - t_{ij,k}^2)$  for the pair  $(u_k, v_k)$ . By definition,  $r_{ij} = \text{rank}(\mathbf{A}_i \mathbf{A}_j^\top) \leq \min(d_{\mathcal{S}_i}, d_{\mathcal{S}_j})$ , we have  $t_{ij,k} = 0$  for all  $k > r_{ij}$ . This indicates that only  $r_{ij}$  canonical coordinates share cross-view information, i.e.,  $\text{SNR} > 0$ , while the remaining modes are independent noise.

To cast this probabilistic correlation structure into a functional-analytic framework, we expand the product bivariate Gaussian density  $\mathcal{K}_{ij}$  in Lemma 1 using normalized multivariate Hermite polynomial as shown in Mehler [1866] and Han et al. [2025].

**Lemma 2** (Normalized Multivariate Mehler-Hermite Expansion). Let  $\{\psi_n\}_{n \geq 0}$  denote the normalized Hermite polynomials of physicist’s form. For a multi-index  $\mathbf{n} \in \mathbb{N}^{r_{ij}}$ , define the normalized multivariate Hermite basis  $\Psi_{\mathbf{n}}(\mathbf{u}) := \prod_{k=1}^{r_{ij}} \psi_{n_k}(u_k)$ , which satisfies the orthonormality condition  $\int_{\mathbb{R}^{r_{ij}}} \phi(\mathbf{u}) \Psi_{\mathbf{n}}(\mathbf{u}) \Psi_{\mathbf{m}}(\mathbf{u}) d\mathbf{u} = \delta_{\mathbf{nm}}$  with  $\delta$  being the Kronecker-delta function, and order- $\mathbf{n}$  canonical correlations  $t_{\mathbf{n}} := \prod_{k=1}^{r_{ij}} t_{ij,k}^{n_k}$ . Then  $\mathcal{K}_{ij}$  admits a multivariate Mehler-Hermite expansion as follows,

$$\mathcal{K}_{ij}(\mathbf{u}, \mathbf{v}) = \phi(\mathbf{u})\phi(\mathbf{v}) \sum_{\mathbf{n} \in \mathbb{N}^{r_{ij}}} t_{\mathbf{n}} \Psi_{\mathbf{n}}(\mathbf{u}) \Psi_{\mathbf{n}}(\mathbf{v}),$$

where  $\phi(\mathbf{u}) = \prod_{k=1}^{r_{ij}} \phi(u_k)$ .

Together with reparameterization invariance (Lemma 6) and whitening-induced canonicalization (Equation 4), Lemma 2 establishes a function-theoretic framework for analyzing the nonlinear representation mappings. By leveraging the orthonormality of Hermite polynomials [Dunkl and Xu, 2014], this framework provides a general technical machinery for isolating nonlinear terms in the representation mappings.

## 5.2 Subspace Identifiability

CCA-like objectives are invariant to within-view invertible transformations, e.g., rotations, that preserve second-order structure after whitening. Since precise recovery of mixing matrices  $\{\mathbf{A}_i\}_{i=1}^N$  is fundamentally impossible, we instead target the basis-invariant signal subspaces they span.

**Definition 1** (Signal and Correlated Subspaces). For each view  $i \in [N]$ , the *signal subspace* is defined as  $\mathcal{U}_i := \text{col}(\mathbf{A}_i) \subseteq \mathbb{R}^{d_{s_i}}$ . For any pair of distinct views  $1 \leq i < j \leq N$ , let  $r_{ij} := \text{rank}(\mathbf{A}_i \mathbf{A}_j^\top)$ . We define the *pairwise correlated subspace* of view  $i$  with respect to view  $j$  as

$$\mathcal{U}_{i|j} := \text{col}(\mathbf{U}_{ij}(:, 1 : r_{ij})), \quad \mathcal{U}_{j|i} := \text{col}(\mathbf{V}_{ij}(:, 1 : r_{ij})).$$

Note that  $\mathcal{U}_{i|j} \subseteq \mathcal{U}_i$  and  $\mathcal{U}_{j|i} \subseteq \mathcal{U}_j$ , with equality holding if and only if  $r_{ij} = \text{rank}(\mathbf{A}_i)$  and  $r_{ij} = \text{rank}(\mathbf{A}_j)$ , respectively. Finally, the *multi-view jointly correlated subspace* for view  $i$  is defined as the intersection of its pairwise correlated subspaces:  $\mathcal{U}_i^{\text{mv}} := \bigcap_{j \neq i} \mathcal{U}_{i|j}$ .

We then give the correlated subspace identifiability in two-view setup.

**Theorem 5.1** (Infinite-Dimensional Two-view Subspace Identifiability). Fix a pair of distinct views  $i \neq j$  and let  $r_{ij} := \text{rank}(\mathbf{A}_i \mathbf{A}_j^\top) \leq d_{\mathcal{Z}}$ . Suppose the observed data are generated by the multi-view generative process defined in Equation 1, where the generative functions  $\mathbf{g}_i$  and  $\mathbf{g}_j$  are smooth and invertible

and Assumption 1 holds. Let  $(\tilde{\mathbf{f}}_i^*, \tilde{\mathbf{f}}_j^*)$  be any whitened population maximizer of the two-view CCA objective in Equation 2, and define the composition mappings  $\tilde{\mathbf{h}}_\ell^* := \tilde{\mathbf{f}}_\ell^* \circ \mathbf{g}_\ell$  for  $\ell \in \{i, j\}$ .

Assuming an infinite feature dimension, i.e.,  $d_{\mathcal{Z}} \rightarrow \infty$ , there exist orthogonal matrices  $\mathbf{O}_i, \mathbf{O}_j \in O(r_{ij})$  such that,

$$\begin{aligned} \mathbf{P}_{r_{ij}} \tilde{\mathbf{h}}_i^*(\mathbf{s}_i) &= \mathbf{O}_i \mathbf{U}_{ij}(:, 1 : r_{ij})^\top \mathbf{W}_i \mathbf{s}_i, \\ \mathbf{P}_{r_{ij}} \tilde{\mathbf{h}}_j^*(\mathbf{s}_j) &= \mathbf{O}_j \mathbf{V}_{ij}(:, 1 : r_{ij})^\top \mathbf{W}_j \mathbf{s}_j, \end{aligned} \quad (7)$$

where  $\mathbf{P}_{r_{ij}}$  is a selection matrix that extracts exactly  $r_{ij}$  coordinates. Consequently, the maximizers identify the  $r_{ij}$ -dimensional whitened correlated subspaces  $\mathcal{U}_{i|j}$  and  $\mathcal{U}_{j|i}$  up to orthogonal transformations.

**Assumption 2** (First-Order Canonical Dominance). For any pair of views  $1 \leq i < j \leq N$  with  $\text{rank}(\mathbf{A}_i \mathbf{A}_j^\top) \geq 2$ , the strictly positive canonical correlations satisfy  $t_{ij,r_{ij}} > t_{ij,1}^2$ .

**Corollary 1** (Finite-Dimensional Two-view Subspace Identifiability). Suppose the conditions of Theorem 5.1 hold, along with the First-Order Dominance condition (Assumption 2). For any finite representation dimension  $d_{\mathcal{Z}} \geq r_{ij}$ , the identifiability guarantees in Equation 7 hold exactly, where the selection matrix takes the explicit form  $\mathbf{P}_{r_{ij}} := [\mathbf{I}_{r_{ij}} \ \mathbf{0}] \in \mathbb{R}^{r_{ij} \times d_{\mathcal{Z}}}$ .

*Remark 2* (Spectral separation of higher-order components). The Mehler-Hermite expansion (Lemma 2) decomposes the cross-view coupling into linear and higher-order (nonlinear) polynomial modes. Assumption 2 mathematically ensures that the weakest linear correlation ( $t_{ij,r_{ij}}$ ) strictly exceeds the strongest possible higher-order correlation, which is bounded by  $t_{ij,1}^2$ . This spectral gap guarantees that in the finite-dimensional regime (Corollary 1), the generalized CCA objective strictly prioritizes the linear components, securely isolating them in the leading  $r_{ij}$  coordinates. Consequently, the remaining trailing dimensions, i.e., those coordinates with indices  $> r_{ij}$ , of the learned representations exclusively capture orthogonal linear combinations of the higher-order nonlinear modes of the whitened sources  $\mathbf{U}_{ij}(:, 1 : r_{ij})^\top \mathbf{W}_i \mathbf{s}_i$  and  $\mathbf{V}_{ij}(:, 1 : r_{ij})^\top \mathbf{W}_j \mathbf{s}_j$ , as demonstrated by Han et al. [2025].

**Theorem 5.2** (Infinite-Dimensional Multi-View Subspace Identifiability). Suppose the conditions of Theorem 5.1 hold for  $N \geq 3$  view ensembles and let  $\{\tilde{\mathbf{f}}_i^*\}_{i=1}^N$  be any whitened population maximizer of the generalized CCA objective in Equation 2. For each view  $i$ , let  $r_i := \dim(\mathcal{U}_i^{\text{mv}})$  and let  $\mathbf{U}_i^{\text{mv}} \in \mathbb{R}^{d_{s_i} \times r_i}$  be an orthonormal basis spanning the multi-view jointly correlated subspace  $\mathcal{U}_i^{\text{mv}}$ .

Assuming an infinite feature dimension, i.e.,  $d_{\mathcal{Z}} \rightarrow \infty$ ,

there exist orthogonal matrices  $\mathbf{O}_i \in O(r_i)$  such that,

$$\mathbf{P}_{r_i} \tilde{\mathbf{h}}_i^*(\mathbf{s}_i) = \mathbf{O}_i (\mathbf{U}_i^{\text{mv}})^\top \mathbf{W}_i \mathbf{s}_i, \quad \forall i \in [N], \quad (8)$$

where  $\mathbf{P}_{r_i}$  is a selection matrix that extracts exactly  $r_i$  coordinates of  $\mathbf{u}$  corresponding to the mutually correlated signals across all views. Consequently, the multi-view maximizers simultaneously identify the multi-view jointly correlated subspaces  $\mathcal{U}_i^{\text{mv}}$  up to view-specific orthogonal transformations.

*Remark 3* (Subspace dimensionality and partial observability). Because the multi-view jointly correlated subspace  $\mathcal{U}_i^{\text{mv}}$  acts as a strict intersection filter, it isolates only those latent signals that are mutually visible across the entire  $N$ -view ensemble. Consequently, its dimension  $r_i$  is strictly bounded by, and typically lower than, the pairwise ranks  $r_{ij}$ . Furthermore, for latent factors shared only among a strict subset of views, the generalized CCA objective lacks sufficient global constraints to enforce alignment, causing the corresponding unshared representation dimensions to inherently drift [Yao et al., 2024b]. The finite-dimensional counterpart of Equation 8 follows analogously to Corollary 1.

### 5.3 Finite-Sample Statistical Consistency

We now quantify the statistical error incurred when replacing population (second-order) moments in Equation 2 by their empirical estimates. Since our identifiability results are driven by the singular/eigenspaces of normalized cross-covariances, the analysis reduces to (i) concentration of empirical covariances in operator norm and (ii) stability of singular/eigenspaces under perturbations.

#### Empirical Normalized Cross-Covariances.

Given  $n$  i.i.d. samples  $\{(\mathbf{x}_1^{(t)}, \dots, \mathbf{x}_N^{(t)})\}_{t=1}^n$  and fixed encoders  $\{\mathbf{f}_i\}_{i=1}^N$ , let  $\mathbf{z}_i^{(t)} := \mathbf{f}_i(\mathbf{x}_i^{(t)})$ . With  $\bar{\mathbf{z}}_i$  and  $\bar{\mathbf{z}}_j$  denoting the empirical means of the representations for views  $i$  and  $j$ , define the sample cross-covariance matrices as  $\hat{\Sigma}_{ij} := \frac{1}{n} \sum_{t=1}^n (\mathbf{z}_i^{(t)} - \bar{\mathbf{z}}_i)(\mathbf{z}_j^{(t)} - \bar{\mathbf{z}}_j)^\top$ . The empirical normalized cross-covariance is

$$\hat{\mathbf{R}}_{ij} := \hat{\Sigma}_{ii}^{-1/2} \hat{\Sigma}_{ij} \hat{\Sigma}_{jj}^{-1/2}, \quad 1 \leq i < j \leq N, \quad (9)$$

with population counterpart  $\mathbf{R}_{ij} := \Sigma_{ii}^{-1/2} \Sigma_{ij} \Sigma_{jj}^{-1/2}$ . Let  $\hat{\mathcal{U}}_{i|j}$  denote the rank- $r_{ij}$  left singular subspace of  $\hat{\mathbf{R}}_{ij}$ . By Corollary 1, this subspace estimates the pairwise correlated subspace  $\mathcal{U}_{i|j}$  up to orthogonal ambiguity.

Additionally, we impose a mild tail condition on the population-whitened representations  $\tilde{\mathbf{z}}_i := \Sigma_{ii}^{-1/2}(\mathbf{z}_i - \mathbb{E}[\mathbf{z}_i])$ .

**Assumption 3** (Sub-Gaussian whitened representations). There exists  $\kappa > 0$  such that for all  $i \in [N]$ ,  $\sup_{\|\mathbf{u}\|_2=1} \|\mathbf{u}^\top \tilde{\mathbf{z}}_i\|_{\psi_2} \leq \kappa$ .

Assumption 3 yields operator-norm concentration for  $\hat{\Sigma}_{ij}$  and controls the error of the empirical whitening factors  $\hat{\Sigma}_{ii}^{-1/2}$ , which together imply concentration of the normalized cross-covariances  $\hat{\mathbf{R}}_{ij}$  in Equation 9. To translate this moment error into a subspace error, we require a spectral separation of the target singular subspaces: for each pair  $(i, j)$ , define  $\Delta_{ij} := \sigma_{r_{ij}}(\mathbf{R}_{ij}) - \sigma_{r_{ij}+1}(\mathbf{R}_{ij}) > 0$ . Under Assumption 2, whenever  $r_{ij} \geq 2$  one has the explicit lower bound  $\Delta_{ij} \geq t_{ij, r_{ij}} - t_{ij, 1}^2$ , reflecting the strict dominance of linear modes over higher-order Mehler-Hermite components. We then give out finite-sample

**Theorem 5.3** (Finite-sample subspace recovery). *Suppose Assumption 3 holds and  $d_{\mathcal{Z}} < \infty$ . Then for any  $\delta \in (0, 1)$ , with probability at least  $1 - \delta$ , simultaneously for all  $1 \leq i < j \leq N$ ,*

$$\|\hat{\mathbf{R}}_{ij} - \mathbf{R}_{ij}\|_2 \leq C \kappa^2 \sqrt{\frac{d_{\mathcal{Z}} + \log(N/\delta)}{n}}, \quad (10)$$

for a universal constant  $C > 0$ . Moreover, on the event  $\|\hat{\mathbf{R}}_{ij} - \mathbf{R}_{ij}\|_2 \leq \Delta_{ij}/2$ ,

$$\|\sin \Theta(\hat{\mathcal{U}}_{i|j}, \mathcal{U}_{i|j})\|_2 \leq \frac{2\|\hat{\mathbf{R}}_{ij} - \mathbf{R}_{ij}\|_2}{\Delta_{ij}}, \quad (11)$$

and the same bound holds for the right singular subspace  $\hat{\mathcal{U}}_{j|i}$ .

*Remark 4* (Scaling with  $n$ ). Combining Equation 10–Equation 11 gives the parametric  $O_{\mathbb{P}}(n^{-1/2})$  rate. In particular,  $\|\sin \Theta\|_2 \leq \varepsilon$  is achieved once  $n \gtrsim \kappa^4 (d_{\mathcal{Z}} + \log(N/\delta)) / (\Delta_{ij}^2 \varepsilon^2)$ .

To recover the multi-view jointly correlated subspace  $\mathcal{U}_i^{\text{mv}}$  from noisy pairwise estimates, we use an averaged-projector intersection filter. Let  $\mathbf{P}_{i|j}$  and  $\hat{\mathbf{P}}_{i|j}$  denote the orthogonal projectors onto  $\mathcal{U}_{i|j}$  and  $\hat{\mathcal{U}}_{i|j}$ , and define

$$\mathbf{S}_i := \frac{1}{N-1} \sum_{j \neq i} \mathbf{P}_{i|j}, \quad \hat{\mathbf{S}}_i := \frac{1}{N-1} \sum_{j \neq i} \hat{\mathbf{P}}_{i|j}.$$

Under Assumption 2,  $\mathcal{U}_i^{\text{mv}}$  is the top- $r_i$  eigenspace of  $\mathbf{S}_i$  by definition. Let the corresponding eigengap be  $\Gamma_i := 1 - \lambda_{r_i+1}(\mathbf{S}_i) > 0$ , and let  $\hat{\mathcal{U}}_i^{\text{mv}}$  be the top- $r_i$  eigenspace of  $\hat{\mathbf{S}}_i$ .

**Corollary 2** (Consistency of the intersection filter). *Under the conditions of Theorem 5.3, with probability at least  $1 - \delta$ , for every  $i \in [N]$ ,*

$$\begin{aligned} \|\sin \Theta(\hat{\mathcal{U}}_i^{\text{mv}}, \mathcal{U}_i^{\text{mv}})\|_2 &\leq \frac{\|\hat{\mathbf{S}}_i - \mathbf{S}_i\|_2}{\Gamma_i} \\ &\leq \frac{2}{\Gamma_i} \max_{j \neq i} \|\sin \Theta(\hat{\mathcal{U}}_{i|j}, \mathcal{U}_{i|j})\|_2. \end{aligned}$$

Consequently,  $\widehat{U}_i^{\text{mv}}$  is consistent at rate  $O_{\mathbb{P}}(n^{-1/2})$ , governed by  $\{\Delta_{ij}\}$  and  $\Gamma_i$ .

All proofs are deferred to the supplementary material.

## 6 Experiments

In this section, we empirically validate our theoretical results using controlled generative experiments designed to assess subspace identifiability under known nonlinear mixing functions. We construct synthetic multi-view settings in which latent factors and spectral conditions can be systematically varied and ablated. Our setup extends established disentanglement learning benchmarks [Zimmermann et al., 2021, Matthes et al., 2023, Han et al., 2025] to the multi-view ( $N = 3$ ) regime considered in this work.

### 6.1 Experimental Setup

**Datasets.** We evaluate on two datasets providing full control over the generative factors:

- **Synthetic Data:** We extend the single-generator setup of Zimmermann et al. [2021] to an  $N = 3$  multi-view regime. Observations are produced by applying independent nonlinear generating functions to view-specific sources sampled from our additive model (Equation 1), enabling exact control over the latent distributions and mixing matrices.
- **3DIdent** [Daunhawer et al., 2023b]: A physically rendered dataset of 3D objects governed by 11 latent factors (e.g., shape, pose, illumination). Since the factors are discrete, we connect 3DIdent to our continuous generative model via nearest-neighbor matching: we sample continuous latent vectors, i.e.,  $\mathbf{s}_1, \mathbf{s}_2$  and  $\mathbf{s}_3$  w.r.t. Equation 1, and map them to the rendered instance whose factor tuple is closest in Euclidean distance, and then generate the three views.

**Construction of Linear Mixing Matrices.** To strictly control the pairwise canonical correlations of  $\mathbf{R}_{ij}$  in Equation 5, we construct the mixing matrices  $\{\mathbf{A}_i\}_{i=1}^3$  to match target singular values  $\{t_{ij,k}\}_{k=1}^{r_{ij}} \subset [0, 1)$  for the population normalized cross-covariance matrices,

$$\mathbf{R}_{ij} = (\mathbf{A}_i \mathbf{A}_i^\top + \mathbf{I})^{-1/2} \mathbf{A}_i \mathbf{A}_j^\top (\mathbf{A}_j \mathbf{A}_j^\top + \mathbf{I})^{-1/2}.$$

By assigning a shared right singular matrix  $\mathbf{P} \in O(d)$  across all  $\mathbf{A}_i$ , the singular values of  $\mathbf{R}_{ij}$  factorize elementwise as  $t_{ij,k} = g_{i,k} g_{j,k}$ , where  $g_{i,k} := \sigma_{i,k} / \sqrt{1 + \sigma_{i,k}^2}$  and  $\sigma_{i,k}$  are the singular values of  $\mathbf{A}_i$ . For  $N = 3$  views, this algebraic system uniquely yields  $g_{i,k} = (t_{ij,k} t_{ki,k} / t_{jk,k})^{1/2}$ , subsequently fixing

$\sigma_{i,k} = g_{i,k} / \sqrt{1 - g_{i,k}^2}$ . We then construct  $\mathbf{A}_i := \mathbf{U}_i \text{diag}(\sigma_{i,1}, \dots, \sigma_{i,r_{ij}}) \mathbf{P}^\top$ , sampling independent random orthogonal matrices  $\mathbf{U}_i \in O(d)$ . This guarantees the exact prescribed canonical spectra while randomizing the signal subspace orientations.

**Baselines.** We benchmark generalized CCA against strong self-supervised learning baselines to test subspace identifiability under a unified encoder architecture and distribution families aligned with our theory:

- **Barlow Twins** [Zbontar et al., 2021]: Enforces invariance and minimizes redundancy through cross-correlation diagonalization.
- **W-MSE** [Ermolov et al., 2021]: Aligns whitened multi-view neural representations by minimizing mean-squared error.
- **InfoNCE** [Oord et al., 2018]: The standard contrastive learning objective, maximizing mutual information between views, shown to be identifiable under mild conditions [Zimmermann et al., 2021, Matthes et al., 2023].
- **Generalized CCA (GCCA)** [Kettenring, 1971]: Maximizes the sum of pairwise CCA objectives in the multi-view setting by utilizing whitened multi-view representations.

To approximate the view-specific encoding functions  $\{\mathbf{f}_i\}_{i=1}^N$ , we parameterize them as neural networks, leveraging their universal approximation capability. We adopt neural-network-parameterized GCCA and treat its converged solution as a surrogate for the population GCCA solution when data are generated via online sampling from the underlying distributions. All baselines are implemented using their official repositories when available, otherwise we re-implement following the authors’ specifications.

**Metrics.** We assess subspace recovery via principal angles between the span of the learned whitened representation and the ground-truth canonical subspace. Specifically, we report the mean principal angle ( $PA_{\text{mean}}$ ) and the maximum principal angle ( $PA_{\text{max}}$ ), following standard subspace identification practice [Ma and Li, 2020, Gao et al., 2017, Cai and Zhang, 2018].

In all experiments, view-specific encoders are trained using Adam with a fixed learning rate of  $10^{-4}$ . The batch size is set to 1024 for synthetic data and 256 for 3DIdent. On the synthetic dataset with  $d_S = 5$ , 100,001 training steps require approximately 2.5 hours, whereas 40,000 steps on 3DIdent take about 20 hours on a single RTX A5000 GPU. All reported results are averaged over five random seeds.

Methods	$\tilde{\mathbf{f}}_1$		$\tilde{\mathbf{f}}_2$		$\tilde{\mathbf{f}}_3$	
	$PA_{\text{mean}}$	$PA_{\text{max}}$	$PA_{\text{mean}}$	$PA_{\text{max}}$	$PA_{\text{mean}}$	$PA_{\text{max}}$
BarlowTwins	34.12 $\pm$ 0.21	86.41 $\pm$ 0.95	31.85 $\pm$ 0.18	81.22 $\pm$ 0.82	33.40 $\pm$ 0.24	84.95 $\pm$ 0.91
InfoNCE	4.95 $\pm$ 0.06	8.15 $\pm$ 0.52	5.12 $\pm$ 0.09	8.42 $\pm$ 0.38	<b>4.88 <math>\pm</math> 0.08</b>	<b>7.98 <math>\pm</math> 0.47</b>
W-MSE	5.08 $\pm$ 0.08	8.31 $\pm$ 0.41	<b>4.91 <math>\pm</math> 0.05</b>	<b>7.95 <math>\pm</math> 0.58</b>	5.03 $\pm$ 0.07	8.24 $\pm$ 0.44
GCCA	<b>4.85 <math>\pm</math> 0.05</b>	<b>7.92 <math>\pm</math> 0.35</b>	4.98 $\pm$ 0.08	8.11 $\pm$ 0.42	4.92 $\pm$ 0.06	8.05 $\pm$ 0.51

Table 1: Comparison of the mean and maximum principal angles ( $PA_{\text{mean}}$ ,  $PA_{\text{max}}$ ) on synthetic data ( $d_{S_i} = d_Z = 5, \forall i \in [3]$ ) under Gaussian prior ( $p_\phi$ ).

Methods	$\tilde{\mathbf{f}}_1$		$\tilde{\mathbf{f}}_2$		$\tilde{\mathbf{f}}_3$	
	$PA_{\text{mean}}$	$PA_{\text{max}}$	$PA_{\text{mean}}$	$PA_{\text{max}}$	$PA_{\text{mean}}$	$PA_{\text{max}}$
BarlowTwins	34.21 $\pm$ 0.45	86.42 $\pm$ 1.85	36.15 $\pm$ 0.52	82.75 $\pm$ 2.15	35.82 $\pm$ 0.61	88.14 $\pm$ 1.92
InfoNCE	8.05 $\pm$ 0.18	11.21 $\pm$ 0.65	8.12 $\pm$ 0.22	10.85 $\pm$ 0.82	7.98 $\pm$ 0.15	11.42 $\pm$ 0.91
W-MSE	8.15 $\pm$ 0.25	10.95 $\pm$ 0.78	7.92 $\pm$ 0.19	11.15 $\pm$ 0.55	8.11 $\pm$ 0.21	10.88 $\pm$ 0.88
GCCA	<b>7.82 <math>\pm</math> 0.16</b>	<b>10.51 <math>\pm</math> 0.62</b>	<b>7.85 <math>\pm</math> 0.18</b>	<b>10.45 <math>\pm</math> 0.71</b>	<b>7.80 <math>\pm</math> 0.15</b>	<b>10.48 <math>\pm</math> 0.68</b>

Table 2: Comparison of the mean and maximum principal angles ( $PA_{\text{mean}}$ ,  $PA_{\text{max}}$ ) on 3DIdent ( $d_{S_i} = d_Z = 11, \forall i \in [3]$ ) under Gaussian prior ( $p_\phi$ ).

## 6.2 Validation of Theoretical Findings

**Subspace Identifiability.** We empirically validate subspace identifiability under our additive generative model in Equation 1. For simplicity, we present the results using Gaussian prior. Results for other admissible non-Gaussian distributions are deferred to the supplementary material. Setting the latent dimensions to  $d_C = d_{S_i} = 5$ , we independently sample the shared content  $\mathbf{c}$  and view-private noise  $\{\epsilon_i\}_{i=1}^N$  from the selected distributions (details in the supplementary material). To invert this process, the view-specific encoders  $\{\mathbf{f}_i\}_{i=1}^N$  are implemented as residual MLPs equipped with batch normalization to ensure stable optimization.

Table 1 and Table 2 report the subspace recovery errors on the synthetic and 3DIdent datasets under the Gaussian prior. GCCA, InfoNCE, and W-MSE achieve consistently low subspace errors across all views, exhibiting tightly bounded mean and maximum principal angles ( $PA_{\text{mean}}$ ,  $PA_{\text{max}}$ ). Notably, GCCA consistently yields the lowest subspace errors, which is consistent with our multi-view identifiability guarantees. Conversely, BarlowTwins fails to properly isolate the jointly correlated subspaces, suffering from severe misalignment ( $PA_{\text{max}} > 80^\circ$ ) in all scenarios. Crucially, these performance hierarchies remain strictly robust when transitioning from the perfectly controlled low-dimensional synthetic regime ( $d_Z = 5$ ) to the visually complex, higher-dimensional 3DIdent environment ( $d_Z = 11$ ).

**Ablation on First-order Canonical Dominance.** Let  $\rho_{d_S}/\rho_1^2$  denote the first-order canonical dominance ratio. We ablate Assumption 2 by varying this ratio while keeping all other parameters fixed. Figure 1 reports the resulting mean and maximum principal

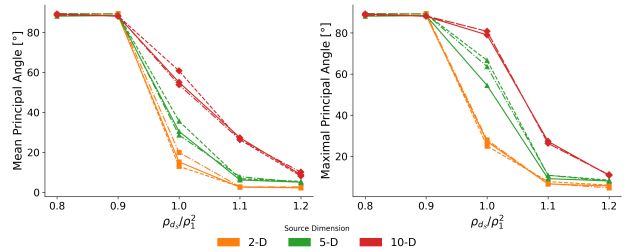


Figure 1: Ablation over the first-order canonical ratio  $\rho_{d_S}/\rho_1^2$  ( $d_S = d_Z$ ). Left and right panels display the mean ( $PA_{\text{mean}} \downarrow$ ) and maximum ( $PA_{\text{max}} \downarrow$ ) principal angles, respectively. Colors indicate source dimensions, while solid, dashed, and dash-dotted lines denote the view-specific encoders  $\tilde{\mathbf{f}}_1$ ,  $\tilde{\mathbf{f}}_2$ , and  $\tilde{\mathbf{f}}_3$ .

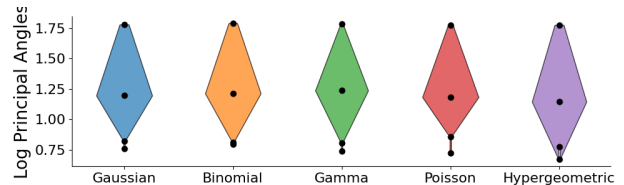


Figure 2: Log principal angles of encoder  $\mathbf{f}_1$  in the under-complete setup ( $d_{S_i} = 5$ ,  $d_Z = 4, \forall i \in [3]$ ). Black dots denote principal angles and the shaded region indicates the log-standard deviation.

angles on synthetic dataset when the source canonical correlations are uniformly sampled from  $[\rho_{d_S}, \rho_1]$ . When  $\rho_{d_S}/\rho_1^2 < 1$ , at least one canonical direction violates the dominance condition, leading to persistently large  $PA_{\text{max}}$  and incomplete subspace recovery. Once the ratio exceeds 1, both  $PA_{\text{mean}}$  and  $PA_{\text{max}}$  decrease sharply, indicating full identifiability of all canonical directions. The transition is more abrupt at lower source dimensions, reflecting more concentrated recoverability in low-dimensional regimes.

Encoder	Gaussian	Binomial	Gamma	Poisson	Hypergeometric
$\tilde{\mathbf{f}}_1$	5.42 $\pm$ 0.08	5.58 $\pm$ 0.12	5.47 $\pm$ 0.05	5.61 $\pm$ 0.14	5.53 $\pm$ 0.09
$\tilde{\mathbf{f}}_2$	5.51 $\pm$ 0.11	5.39 $\pm$ 0.07	5.65 $\pm$ 0.15	5.48 $\pm$ 0.06	5.55 $\pm$ 0.10
$\tilde{\mathbf{f}}_3$	5.45 $\pm$ 0.09	5.62 $\pm$ 0.13	5.50 $\pm$ 0.08	5.41 $\pm$ 0.11	5.59 $\pm$ 0.07

Table 3: Mean principal angle ( $PA_{\text{mean}} \downarrow$ ) in the over-complete regime ( $d_{S_i} = 5$ ,  $d_Z = 7, \forall i \in [3]$ ).

**Ablation on Dimension Mismatch.** We study identifiability under dimension mismatch on synthetic dataset. In the under-complete regime ( $d_S > d_Z$ ), Figure 2 shows the log-principal-angle distribution across source distributions. Across all cases, several directions attain small angles, while at least one direction remains bounded away from zero, indicating partial but not full subspace recovery. The variability is lim-

---

ited, suggesting robustness to distributional choice, yet the missing dimension prevents complete identifiability.

In the over-complete regime ( $d_S < d_Z$ ), Table 3 reports consistently high  $R^2$ , confirming recovery of the source subspace up to redundant coordinates. However, although our theory suggests that redundant latent dimensions encode higher-order components of the canonical coordinates, this effect is not explicitly isolated in our current experiments. Consequently, excess dimensions do not yield unique identification, and no global identifiability guarantee can be established under dimension mismatch. Future work will investigate this higher-order structure more systematically.

## 7 Discussion and Conclusion

We reframed nonlinear multi-view CCA as a basis-invariant subspace identification problem. By considering an additive multi-view generative process, we proved that for  $N \geq 3$  views, generalized CCA acts as a provable intersection filter, isolating jointly correlated signal subspaces while discarding view-private noise up to an orthogonal ambiguity. The First-Order Canonical Dominance condition theoretically guarantees the spectral separation of linear signals from higher-order nonlinearities via a multivariate Mehler–Hermite expansion. This spectral gap subsequently enables finite-sample subspace recovery via finite-dimensional representation.

While our theory assumes exact dimensional matching and full-rank source, experiments demonstrate the behavior of CCA in capacity-mismatched regimes. Future work will systematically investigate the geometric isolation of higher-order Hermite components in these redundant dimensions, and extend this identifiability framework to rank-deficient source structures, e.g., partial observability, further bridging multivariate statistics with self-supervised learning.

## References

- Kartik Ahuja, Jason S Hartford, and Yoshua Bengio. Weakly supervised representation learning with sparse perturbations. *Advances in Neural Information Processing Systems*, 35:15516–15528, 2022.
- Horace B Barlow, Tej P Kaushal, and Graeme J Mitchison. Finding minimum entropy codes. *Neural computation*, 1(3):412–423, 1989.
- T Tony Cai and Anru Zhang. Rate-optimal perturbation bounds for singular subspaces with applications to high-dimensional statistics. 2018.
- J-F Cardoso. Blind signal separation: statistical principles. *Proceedings of the IEEE*, 86(10):2009–2025, 1998.
- Pierre Comon. Independent component analysis, a new concept? *Signal processing*, 36(3):287–314, 1994.
- Imant Daunhawer, Alice Bizeul, Emanuele Palumbo, Alexander Marx, and Julia E Vogt. Identifiability results for multimodal contrastive learning. *arXiv preprint arXiv:2303.09166*, 2023a.
- Imant Daunhawer, Alice Bizeul, Emanuele Palumbo, Alexander Marx, and Julia E. Vogt. Identifiability results for multimodal contrastive learning. In *International Conference on Learning Representations*, 2023b. URL [https://openreview.net/forum?id=U\\_2kuqoTcB](https://openreview.net/forum?id=U_2kuqoTcB).
- Charles F Dunkl and Yuan Xu. *Orthogonal polynomials of several variables*. Number 155. Cambridge University Press, 2014.
- Geoffrey Kennedy Eagleson. Polynomial expansions of bivariate distributions. *The Annals of Mathematical Statistics*, 35(3):1208–1215, 1964.
- Aleksandr Ermolov, Aliaksandr Siarohin, Enver Sangineto, and Nicu Sebe. Whitening for self-supervised representation learning. In *International conference on machine learning*, pages 3015–3024. PMLR, 2021.
- Borja Rodriguez Gálvez, Arno Blaas, Pau Rodríguez, Adam Golinski, Xavier Suau, Jason Ramapuram, Dan Busbridge, and Luca Zappella. The role of entropy and reconstruction in multi-view self-supervised learning. In *International Conference on Machine Learning*, pages 29143–29160. PMLR, 2023.
- Chao Gao, Zongming Ma, and Harrison H Zhou. Sparse cca: Adaptive estimation and computational barriers. 2017.
- Luigi Gresele, Paul K. Rubenstein, Arash Mehrjou, Francesco Locatello, and Bernhard Schölkopf. The incomplete rosetta stone problem: Identifiability results for multi-view nonlinear ica. In Ryan P.

- 
- Adams and Vibhav Gogate, editors, *Proceedings of The 35th Uncertainty in Artificial Intelligence Conference*, volume 115 of *Proceedings of Machine Learning Research*, pages 217–227. PMLR, 22–25 Jul 2020. URL <https://proceedings.mlr.press/v115/gresele20a.html>.
- Zhiwei Han, Stefan Matthes, and Hao Shen. Provable affine identifiability of nonlinear cca under latent distributional priors. *arXiv preprint arXiv:2510.04758*, 2025.
- Bobby He and Mete Ozay. Exploring the gap between collapsed & whitened features in self-supervised learning. In *International Conference on Machine Learning*, pages 8613–8634. PMLR, 2022.
- Patrik Hoyer, Dominik Janzing, Joris M Mooij, Jonas Peters, and Bernhard Schölkopf. Nonlinear causal discovery with additive noise models. *Advances in neural information processing systems*, 21, 2008.
- Aapo Hyvarinen and Hiroshi Morioka. Unsupervised feature extraction by time-contrastive learning and nonlinear ica. *Advances in neural information processing systems*, 29, 2016.
- Aapo Hyvarinen and Hiroshi Morioka. Nonlinear ica of temporally dependent stationary sources. In *Artificial intelligence and statistics*, pages 460–469. PMLR, 2017.
- Aapo Hyvärinen and Petteri Pajunen. Nonlinear independent component analysis: Existence and uniqueness results. *Neural networks*, 12(3):429–439, 1999.
- Aapo Hyvarinen, Hiroaki Sasaki, and Richard Turner. Nonlinear ica using auxiliary variables and generalized contrastive learning. In *The 22nd international conference on artificial intelligence and statistics*, pages 859–868. PMLR, 2019.
- András Kalapos and Bálint Gyires-Tóth. Whitening consistently improves self-supervised learning. In *2024 International Conference on Machine Learning and Applications (ICMLA)*, pages 448–453. IEEE, 2024.
- Jon R Kettenring. Canonical analysis of several sets of variables. *Biometrika*, 58(3):433–451, 1971.
- Ilyes Khemakhem, Diederik Kingma, Ricardo Monti, and Aapo Hyvarinen. Variational autoencoders and nonlinear ica: A unifying framework. In *International conference on artificial intelligence and statistics*, pages 2207–2217. PMLR, 2020.
- Henry Oliver Lancaster. The structure of bivariate distributions. *The Annals of Mathematical Statistics*, 29(3):719–736, 1958.
- Francesco Locatello, Stefan Bauer, Mario Lucic, Gunnar Raetsch, Sylvain Gelly, Bernhard Schölkopf, and Olivier Bachem. Challenging common assumptions in the unsupervised learning of disentangled representations. In *international conference on machine learning*, pages 4114–4124. PMLR, 2019.
- Francesco Locatello, Ben Poole, Gunnar Rätsch, Bernhard Schölkopf, Olivier Bachem, and Michael Tschannen. Weakly-supervised disentanglement without compromises. In *International conference on machine learning*, pages 6348–6359. PMLR, 2020.
- Qi Lyu and Xiao Fu. Nonlinear multiview analysis: Identifiability and neural network-assisted implementation. *IEEE Transactions on Signal Processing*, 68:2697–2712, 2020.
- Qi Lyu and Xiao Fu. Provable subspace identification under post-nonlinear mixtures. *Advances in Neural Information Processing Systems*, 35:1554–1567, 2022.
- Qi Lyu, Xiao Fu, Weiran Wang, and Songtao Lu. Understanding latent correlation-based multiview learning and self-supervision: An identifiability perspective. *arXiv preprint arXiv:2106.07115*, 2021.
- Zhuang Ma and Xiaodong Li. Subspace perspective on canonical correlation analysis: Dimension reduction and minimax rates. 2020.
- Stefan Matthes, Zhiwei Han, and Hao Shen. Towards a unified framework of contrastive learning for disentangled representations. *Advances in Neural Information Processing Systems*, 36:67459–67470, 2023.
- F Gustav Mehler. Ueber die entwicklung einer function von beliebig vielen variablen nach laplaceschen functionen höherer ordnung. 1866.
- Joris M Mooij, Dominik Janzing, Tom Heskes, and Bernhard Schölkopf. On causal discovery with cyclic additive noise models. *Advances in neural information processing systems*, 24, 2011.
- Aaron van den Oord, Yazhe Li, and Oriol Vinyals. Representation learning with contrastive predictive coding. *arXiv preprint arXiv:1807.03748*, 2018.
- Teodora Pandeva and Patrick Forré. Multi-view independent component analysis with shared and individual sources. In *Uncertainty in Artificial Intelligence*, pages 1639–1650. PMLR, 2023.
- Gunwoong Park. Identifiability of additive noise models using conditional variances. *Journal of Machine Learning Research*, 21(75):1–34, 2020.
- Jonas Peters, Dominik Janzing, and Bernhard Schölkopf. Causal inference on discrete data using additive noise models. *IEEE Transactions on Pattern Analysis and Machine Intelligence*, 33(12):2436–2450, 2011.

- 
- Anastasia Podosinnikova, Francis Bach, and Simon Lacoste-Julien. Beyond cca: Moment matching for multi-view models. In Maria Florina Balcan and Kilian Q. Weinberger, editors, *Proceedings of the 33rd International Conference on Machine Learning*, volume 48 of *Proceedings of Machine Learning Research*, pages 458–467, New York, New York, USA, 20–22 Jun 2016. PMLR. URL <https://proceedings.mlr.press/v48/podosinnikova16.html>.
- Bernhard Schölkopf, David W Hogg, Dun Wang, Daniel Foreman-Mackey, Dominik Janzing, Carl-Johann Simon-Gabriel, and Jonas Peters. Modeling confounding by half-sibling regression. *Proceedings of the National Academy of Sciences*, 113(27):7391–7398, 2016.
- Rui Shu, Yining Chen, Abhishek Kumar, Stefano Ermon, and Ben Poole. Weakly supervised disentanglement with guarantees. *arXiv preprint arXiv:1910.09772*, 2019.
- Nils Sturma, Chandler Squires, Mathias Drton, and Caroline Uhler. Unpaired multi-domain causal representation learning. *Advances in Neural Information Processing Systems*, 36:34465–34492, 2023.
- Julius Von Kügelgen, Yash Sharma, Luigi Gresele, Wieland Brendel, Bernhard Schölkopf, Michel Besserve, and Francesco Locatello. Self-supervised learning with data augmentations provably isolates content from style. *Advances in neural information processing systems*, 34:16451–16467, 2021.
- Xi Weng, Lei Huang, Lei Zhao, Rao Anwer, Salman H Khan, and Fahad Shahbaz Khan. An investigation into whitening loss for self-supervised learning. *Advances in Neural Information Processing Systems*, 35:29748–29760, 2022.
- Danru Xu, Dingling Yao, Sébastien Lachapelle, Perouz Taslakian, Julius Von Kügelgen, Francesco Locatello, and Sara Magliacane. A sparsity principle for partially observable causal representation learning. In *Proceedings of the 41st International Conference on Machine Learning*, pages 55389–55433, 2024.
- Dingling Yao, Dario Rancati, Riccardo Cadei, Marco Fumero, and Francesco Locatello. Unifying causal representation learning with the invariance principle. *arXiv preprint arXiv:2409.02772*, 2024a.
- Dingling Yao, Danru Xu, Sébastien Lachapelle, Sara Magliacane, Perouz Taslakian, Georg Martius, Julius von Kügelgen, and Francesco Locatello. Multi-view causal representation learning with partial observability. In *The Twelfth International Conference on Learning Representations*, 2024b. URL <https://openreview.net/forum?id=OGtnhKQJms>.
- Jure Zbontar, Li Jing, Ishan Misra, Yann LeCun, and Stéphane Deny. Barlow twins: Self-supervised learning via redundancy reduction. In *International conference on machine learning*, pages 12310–12320. PMLR, 2021.
- Roland S Zimmermann, Yash Sharma, Steffen Schneider, Matthias Bethge, and Wieland Brendel. Contrastive learning inverts the data generating process. In *International conference on machine learning*, pages 12979–12990. PMLR, 2021.

# Supplementary Material

March 2, 2026

## 8 Auxiliary Tools from Prior Works

### 8.1 Reparameterization Invariance

**Definition 2** (Whitened Encoder Classes with Post-orthogonal Closure). Let  $\mathcal{H}_{\mathcal{X}} \subset L^2(P_{\mathbf{x}}; \mathbb{R}^{d_{\mathcal{Z}}})$  be Hilbert spaces of square-integrable vector-valued functions. For base encoders  $\forall \mathbf{f} \in \mathcal{H}_{\mathcal{X}}$  with covariance matrix  $\Sigma_{\mathbf{f}}$  symmetric positive definite, choose any  $\mathbf{W}_{\mathbf{f}} \in \text{GL}(d_{\mathcal{Z}})$  such that  $\mathbf{W}_{\mathbf{f}} \Sigma_{\mathbf{f}} \mathbf{W}_{\mathbf{f}}^{\top} = \mathbf{I}_{d_{\mathcal{Z}}}$ . Define the whitened encoder class on domain  $\mathcal{X}$  by

$$\tilde{\mathcal{F}}_{\mathcal{X}} := \left\{ \mathbf{W}_{\mathbf{f}}(\mathbf{f} - \mathbb{E}[\mathbf{f}(\mathbf{x})]) : \mathbf{f} \in \mathcal{H}_{\mathcal{X}}, \Sigma_{\mathbf{f}} \succ 0 \right\},$$

and  $\mathbf{Q}\tilde{\mathbf{f}} \in \tilde{\mathcal{F}}_{\mathcal{X}}, \forall \tilde{\mathbf{f}} \in \tilde{\mathcal{F}}_{\mathcal{X}}, \mathbf{Q} \in O(d_{\mathcal{Z}})$ . Analogously, we define whitened encoder class  $\tilde{\mathcal{F}}_{\mathcal{X}'}$ , for all base encoders  $\mathbf{f}' \in \mathcal{H}_{\mathcal{X}'} \subset L^2(P_{\mathbf{x}'}; \mathbb{R}^{d_{\mathcal{Z}}})$ .

**Lemma 3** (Pushforward identities and whitening preservation). *Let ground-truth latent pair  $(\mathbf{s}, \mathbf{s}')$  be square-integrable random vectors on  $\mathcal{S} \times \mathcal{S}$  with joint law  $P_{\mathbf{ss}'}$ . Let  $\mathbf{g} : \mathcal{S} \rightarrow \mathcal{X}$  and  $\mathbf{g}' : \mathcal{S} \rightarrow \mathcal{X}'$  be Borel-measurable and observation pair  $(\mathbf{x}, \mathbf{x}') = (g(\mathbf{s}), g'(\mathbf{s}'))$  with joint law  $P_{\mathbf{xx}'} = (\mathbf{g}, \mathbf{g}')_{\#} P_{\mathbf{ss}'}$ . Then the following properties hold.*

1. **Square-integrability.** *For any Borel-measurable  $\tilde{\mathbf{f}} \in \tilde{\mathcal{F}}_{\mathcal{X}}$  with finite second moments on  $\mathcal{X}$ , the composition  $\tilde{\mathbf{f}} \circ \mathbf{g}$  also have finite second moments on  $\mathcal{S}$ . Analogously, the same property also applies to all  $\tilde{\mathbf{f}}' \in \tilde{\mathcal{F}}_{\mathcal{X}'}$ .*
2. **Expectation and Covariance Preservation.** *For all square-integrable  $\tilde{\mathbf{f}} \in \tilde{\mathcal{F}}_{\mathcal{X}}, \tilde{\mathbf{f}}' \in \tilde{\mathcal{F}}_{\mathcal{X}'}$ ,*

$$\begin{aligned} \mathbb{E}[\tilde{\mathbf{f}}(\mathbf{x})] &= \mathbb{E}[\tilde{\mathbf{f}} \circ \mathbf{g}(\mathbf{s})], & \mathbb{E}[\tilde{\mathbf{f}}'(\mathbf{x}')] &= \mathbb{E}[\tilde{\mathbf{f}}' \circ \mathbf{g}'(\mathbf{s}')], \\ \text{Cov}(\tilde{\mathbf{f}}(\mathbf{x})) &= \text{Cov}(\tilde{\mathbf{f}} \circ \mathbf{g}(\mathbf{s})), & \text{Cov}(\tilde{\mathbf{f}}'(\mathbf{x}')) &= \text{Cov}(\tilde{\mathbf{f}}' \circ \mathbf{g}'(\mathbf{s}')), \\ \text{Cov}(\tilde{\mathbf{f}}(\mathbf{x}), \tilde{\mathbf{f}}'(\mathbf{x}')) &= \text{Cov}(\tilde{\mathbf{f}} \circ \mathbf{g}(\mathbf{s}), \tilde{\mathbf{f}}' \circ \mathbf{g}'(\mathbf{s}')). \end{aligned}$$

3. **Whitening Preservation.** *If  $\tilde{\mathbf{f}} \in \tilde{\mathcal{F}}_{\mathcal{X}}$  and  $\tilde{\mathbf{f}}' \in \tilde{\mathcal{F}}_{\mathcal{X}'}$  are whitened with respect to  $P_{\mathbf{x}}$  and  $P_{\mathbf{x}'}$ , respectively. Then  $\tilde{\mathbf{f}} \circ \mathbf{g}$  and  $\tilde{\mathbf{f}}' \circ \mathbf{g}'$  are whitened under  $P_{\mathbf{s}}$  and  $P_{\mathbf{s}'}$ .*

*Proof.*

#### 1. Square-integrability.

Let  $\tilde{\mathbf{f}} \in \tilde{\mathcal{F}}_{\mathcal{X}}, \tilde{\mathbf{f}}' \in \tilde{\mathcal{F}}_{\mathcal{X}'}$  be Borel-measurable and square-integrable under  $P_{\mathbf{x}}$  and  $P_{\mathbf{x}'}$ , respectively. That is,

$$\int_{\mathcal{X}} \|\tilde{\mathbf{f}}(\mathbf{a})\|^2 dP_{\mathbf{x}}(\mathbf{a}) < \infty, \quad \int_{\mathcal{X}'} \|\tilde{\mathbf{f}}'(\mathbf{a})\|^2 dP_{\mathbf{x}'}(\mathbf{a}) < \infty.$$

Because  $P_{\mathbf{x}} = \mathbf{g}_{\#} P_{\mathbf{s}}$  and  $P_{\mathbf{x}'} = \mathbf{g}'_{\#} P_{\mathbf{s}'}$  are the pushforward measure of  $P_{\mathbf{s}}$  and  $P_{\mathbf{s}'}$ . The pushforward identity gives, for any nonnegative measurable  $\varphi \in L^1(P_{\mathbf{x}}), \psi \in L^1(P_{\mathbf{x}'})$ ,

$$\int_{\mathcal{X}} \varphi(\mathbf{a}) dP_{\mathbf{x}}(\mathbf{a}) = \int_{\mathcal{S}} (\varphi \circ \mathbf{g})(\mathbf{b}) dP_{\mathbf{s}}(\mathbf{b}) \quad \text{and} \quad \int_{\mathcal{X}'} \psi(\mathbf{a}) dP_{\mathbf{x}'}(\mathbf{a}) = \int_{\mathcal{S}} (\psi \circ \mathbf{g}')( \mathbf{b}) dP_{\mathbf{s}'}(\mathbf{b}). \quad (12)$$

Applying this to  $\varphi(\mathbf{x}) = \|\mathbf{f}(\mathbf{x})\|^2$  yields

$$\begin{aligned}\mathbb{E}[\|(\tilde{\mathbf{f}} \circ \mathbf{g})(\mathbf{s})\|^2] &= \int_{\mathcal{S}} \|(\tilde{\mathbf{f}} \circ \mathbf{g})(\mathbf{a})\|^2 dP_{\mathbf{s}}(\mathbf{a}) = \int_{\mathcal{X}} \|\tilde{\mathbf{f}}(\mathbf{a})\|^2 dP_{\mathbf{x}}(\mathbf{a}) < \infty, \\ \mathbb{E}[\|(\tilde{\mathbf{f}}' \circ \mathbf{g}')(\mathbf{s}')\|^2] &= \int_{\mathcal{S}'} \|(\tilde{\mathbf{f}}' \circ \mathbf{g}')(\mathbf{b})\|^2 dP_{\mathbf{s}'}(\mathbf{b}) = \int_{\mathcal{X}'} \|\tilde{\mathbf{f}}'(\mathbf{b})\|^2 dP_{\mathbf{x}'}(\mathbf{b}) < \infty.\end{aligned}$$

Thus  $\tilde{\mathbf{f}} \circ \mathbf{g} \in L^2(P_{\mathbf{s}}; \mathbb{R}^{dz})$  and  $\tilde{\mathbf{f}}' \circ \mathbf{g}' \in L^2(P_{\mathbf{s}'}; \mathbb{R}^{dz})$ , as claimed.

## 2. Expectation and covariance preservation.

Let  $\tilde{\mathbf{f}} \in \tilde{\mathcal{F}}_{\mathcal{X}}$ ,  $\tilde{\mathbf{f}}' \in \tilde{\mathcal{F}}_{\mathcal{X}'}$  be Borel and square-integrable under  $P_{\mathbf{x}}$  and  $P_{\mathbf{x}'}$ , respectively.

*Expectations.* Apply Equation 12 componentwise with  $\varphi = \tilde{\mathbf{f}}_j$  and  $\psi = \tilde{\mathbf{f}}'_j$ :

$$\mathbb{E}[\tilde{\mathbf{f}}(\mathbf{x})] = \mathbb{E}[(\tilde{\mathbf{f}} \circ \mathbf{g})(\mathbf{s})], \quad \mathbb{E}[\tilde{\mathbf{f}}'(\mathbf{x}')] = \mathbb{E}[(\tilde{\mathbf{f}}' \circ \mathbf{g}')(\mathbf{s}')].$$

*Second moments and (marginal) covariances.* Using Equation 12 with  $\varphi(\mathbf{x}) = \tilde{\mathbf{f}}(\mathbf{x})\tilde{\mathbf{f}}(\mathbf{x})^\top$  (integrable by Cauchy-Schwarz),  $\forall i, j \in [1, \dots, dz]$ ,

$$\mathbb{E}[\tilde{\mathbf{f}}(\mathbf{x})\tilde{\mathbf{f}}(\mathbf{x})^\top] = \mathbb{E}[(\tilde{\mathbf{f}} \circ \mathbf{g})(\mathbf{s})(\tilde{\mathbf{f}} \circ \mathbf{g})(\mathbf{s})^\top].$$

Subtracting outer products of the means yields

$$\text{Cov}(\tilde{\mathbf{f}}(\mathbf{x})) = \mathbb{E}[\tilde{\mathbf{f}}(\mathbf{x})\tilde{\mathbf{f}}(\mathbf{x})^\top] - \mathbb{E}[\tilde{\mathbf{f}}(\mathbf{x})]\mathbb{E}[\tilde{\mathbf{f}}(\mathbf{x})]^\top = \text{Cov}((\tilde{\mathbf{f}} \circ \mathbf{g})(\mathbf{s})).$$

The same argument applies to  $\tilde{\mathbf{f}}'$ :

$$\text{Cov}(\tilde{\mathbf{f}}'(\mathbf{x}')) = \text{Cov}((\tilde{\mathbf{f}}' \circ \mathbf{g}')(\mathbf{s}')).$$

*Cross-covariances.* For the joint law  $P_{\mathbf{xx}'} = (\mathbf{g}, \mathbf{g}')_{\#} P_{\mathbf{ss}'}$  and any integrable  $\Phi : \mathcal{X} \times \mathcal{X}' \rightarrow \mathbb{R}$ , the well-established generalization of the pushforward measure to joint mappings is as follows:

$$\int_{\mathcal{X} \times \mathcal{X}'} \Phi(\mathbf{a}, \mathbf{b}) dP_{\mathbf{xx}'}(\mathbf{a}, \mathbf{b}) = \int_{\mathcal{S} \times \mathcal{S}'} \Phi(\mathbf{g}(\mathbf{c}), \mathbf{g}'(\mathbf{d})) dP_{\mathbf{ss}'}(\mathbf{c}, \mathbf{d}). \quad (13)$$

By Equation 13 with the matrix-valued integrand  $\Phi(\mathbf{x}) = \tilde{\mathbf{f}}(\mathbf{x})\tilde{\mathbf{f}}'(\mathbf{x}')^\top$  (integrable by Cauchy-Schwarz),  $\forall i, j \in [1, \dots, dz]$ ,

$$\mathbb{E}[\tilde{\mathbf{f}}(\mathbf{x})\tilde{\mathbf{f}}'(\mathbf{x}')^\top] = \mathbb{E}[(\tilde{\mathbf{f}} \circ \mathbf{g})(\mathbf{s})(\tilde{\mathbf{f}}' \circ \mathbf{g}')(\mathbf{s}')^\top].$$

Subtracting the product of means (already matched above) gives

$$\text{Cov}(\tilde{\mathbf{f}}(\mathbf{x}), \tilde{\mathbf{f}}'(\mathbf{x}')) = \text{Cov}((\tilde{\mathbf{f}} \circ \mathbf{g})(\mathbf{s}), (\tilde{\mathbf{f}}' \circ \mathbf{g}')(\mathbf{s}')).$$

All three identities are thus established.

**3. Whitening preservation.** If  $\mathbb{E}[\tilde{\mathbf{f}}(\mathbf{x})] = \mathbf{0}$  and  $\text{Cov}(\tilde{\mathbf{f}}(\mathbf{x})) = \mathbf{I}$ , then by step 2, we get  $\mathbb{E}[\tilde{\mathbf{f}} \circ \mathbf{g}(\mathbf{s})] = \mathbf{0}$  and  $\text{Cov}(\tilde{\mathbf{f}} \circ \mathbf{g}(\mathbf{s})) = \mathbf{I}$ . The argument for  $\tilde{\mathbf{f}}'$  is identical.  $\square$

**Lemma 4** (Bijection under composition). *Let  $\mathcal{S}, \mathcal{X}, \mathcal{X}'$  be standard Borel spaces and  $\mathbf{g}, \mathbf{g}'$  be Borel-measurable and injective. Assume the pushforward measures  $P_{\mathbf{x}} = \mathbf{g}_{\#} P_{\mathbf{s}}$  and  $P_{\mathbf{x}'} = \mathbf{g}'_{\#} P_{\mathbf{s}'}$ . Define the whitened representable latent classes as in Definition 2. Then:*

1. *Composition isometries.* The composition operators

$$\begin{aligned}C_{\mathbf{g}} : L^2(P_{\mathbf{x}}; \mathbb{R}^{dz}) &\rightarrow L^2(P_{\mathbf{s}}; \mathbb{R}^{dz}), & \tilde{\mathbf{f}} &\mapsto \tilde{\mathbf{f}} \circ \mathbf{g}, \\ C_{\mathbf{g}'} : L^2(P_{\mathbf{x}'}; \mathbb{R}^{dz}) &\rightarrow L^2(P_{\mathbf{s}'}; \mathbb{R}^{dz}), & \tilde{\mathbf{f}}' &\mapsto \tilde{\mathbf{f}}' \circ \mathbf{g}',\end{aligned}$$

are linear isometries.

2. **Bijection on whitened classes.** The map

$$\Psi : \tilde{\mathcal{F}}_{\mathcal{X}} \times \tilde{\mathcal{F}}'_{\mathcal{X}'} \longrightarrow \tilde{\mathcal{F}}_{\mathcal{S}} \times \tilde{\mathcal{F}}'_{\mathcal{S}'}, \quad (\tilde{\mathbf{f}}, \tilde{\mathbf{f}}') \longmapsto (\tilde{\mathbf{f}} \circ \mathbf{g}, \tilde{\mathbf{f}}' \circ \mathbf{g}')$$

is a bijection (modulo null sets), with inverse

$$\Psi^{-1} : (\tilde{\mathbf{h}}, \tilde{\mathbf{h}}') \longmapsto (\tilde{\mathbf{h}} \circ \mathbf{g}^{-1}, \tilde{\mathbf{h}}' \circ \mathbf{g}'^{-1}),$$

where  $\mathbf{g}^{-1}$  and  $\mathbf{g}'^{-1}$  are the Borel inverses on the Borel images  $\mathbf{g}(\mathcal{S})$  and  $\mathbf{g}'(\mathcal{S}')$ , respectively. For any  $Q, Q' \in O(d_{\mathcal{Z}})$ ,

$$\Psi(Q\tilde{\mathbf{f}}, Q'\tilde{\mathbf{f}}') = (Q(\tilde{\mathbf{f}} \circ \mathbf{g}), Q'(\tilde{\mathbf{f}}' \circ \mathbf{g}')).$$

*Proof.*

**1. Isometry.**

Since  $\forall \tilde{\mathbf{f}} \in \tilde{\mathcal{F}}_{\mathcal{X}}$ ,

$$\|\tilde{\mathbf{f}} \circ \mathbf{g}\|_{L^2(P_{\mathbf{s}})}^2 = \int_{\mathcal{S}} \|(\tilde{\mathbf{f}} \circ \mathbf{g})(\mathbf{s})\|^2 dP_{\mathbf{s}}(\mathbf{s}) = \int_{\mathcal{X}} \|\tilde{\mathbf{f}}(\mathbf{x})\|^2 d(\mathbf{g}_{\#}P_{\mathbf{s}})(\mathbf{x}) = \|\tilde{\mathbf{f}}\|_{L^2(P_{\mathbf{x}})}^2,$$

so  $C_{\mathbf{g}}$  is a linear isometry. The argument for  $C_{\mathbf{g}'}$  is identical.

**2. Measurable inverses on images.**

Since  $\mathcal{S}, \mathcal{X}$  are standard Borel and  $\mathbf{g}$  is Borel and injective, the Lusin-Souslin theorem implies  $\mathbf{g}(\mathcal{S})$  is Borel in  $\mathcal{X}$  and  $\mathbf{g}^{-1} : \mathbf{g}(\mathcal{S}) \rightarrow \mathcal{S}$  is Borel. The same holds for  $\mathbf{g}'$ .

**3. Surjectivity.**

Let  $\tilde{\mathbf{h}} \in \tilde{\mathcal{F}}_{\mathcal{S}}$ . Define  $\tilde{\mathbf{f}} := \tilde{\mathbf{h}} \circ \mathbf{g}^{-1}$  on  $\mathbf{g}(\mathcal{S})$  and extend arbitrarily to a Borel function on  $\mathcal{X}$ . Then, by Step 2,  $\tilde{\mathbf{f}} \in \tilde{\mathcal{F}}_{\mathcal{X}}$  and  $(\tilde{\mathbf{f}} \circ \mathbf{g})(s) = \tilde{\mathbf{h}}(s)$ . The same construction gives the primed component. Thus  $\Psi$  is surjective

**4. Injectivity.**

If  $\Phi(\tilde{\mathbf{f}}_1, \tilde{\mathbf{f}}'_1) = \Phi(\tilde{\mathbf{f}}_2, \tilde{\mathbf{f}}'_2)$ , then  $\tilde{\mathbf{f}}_1 \circ \mathbf{g} = \tilde{\mathbf{f}}_2 \circ \mathbf{g}$ , hence  $\tilde{\mathbf{f}}_1 = \tilde{\mathbf{f}}_2$ . by applying  $\mathbf{g}^{-1}$  on  $\mathbf{g}(\mathcal{S})$ ; similarly for the primed side. Therefore  $\Psi$  is injective.

Combining the steps yields the stated bijection and properties.  $\square$

**Lemma 5** (Continuity of the Whitening Map). *Let  $\{\mathbf{f}_n\}_{n \geq 1} \subset L^2(P_{\mathbf{x}}; \mathbb{R}^{d_{\mathcal{Z}}})$  be a sequence of square-integrable vector-valued functions such that  $\mathbf{f}_n \rightarrow \mathbf{f}$  in  $L^2(P_{\mathbf{x}})$ . Denote*

$$\boldsymbol{\mu}_n := \mathbb{E}[\mathbf{f}_n(\mathbf{x})], \quad \boldsymbol{\mu} := \mathbb{E}[\mathbf{f}(\mathbf{x})], \quad \boldsymbol{\Sigma}_{\mathbf{f}_n} := \text{Cov}(\mathbf{f}_n(\mathbf{x})), \quad \boldsymbol{\Sigma}_{\mathbf{f}} := \text{Cov}(\mathbf{f}(\mathbf{x})).$$

Assume  $\boldsymbol{\Sigma}_{\mathbf{f}} \succ 0$ , and let

$$\mathbf{W}_{\mathbf{f}_n} := \boldsymbol{\Sigma}_{\mathbf{f}_n}^{-1/2}, \quad \mathbf{W}_{\mathbf{f}} := \boldsymbol{\Sigma}_{\mathbf{f}}^{-1/2}.$$

Then, for all  $n$  sufficiently large,  $\boldsymbol{\Sigma}_{\mathbf{f}_n} \succ 0$  and

$$\mathbf{W}_{\mathbf{f}_n}(\mathbf{f}_n - \boldsymbol{\mu}_n) \xrightarrow[n \rightarrow \infty]{L^2} \mathbf{W}_{\mathbf{f}}(\mathbf{f} - \boldsymbol{\mu}). \quad (14)$$

Moreover, if  $\mathbf{U}_{\mathbf{f}_n} \in \text{GL}(d_{\mathcal{Z}})$  are any whiteners satisfying  $\mathbf{U}_{\mathbf{f}_n} \boldsymbol{\Sigma}_{\mathbf{f}_n} \mathbf{U}_{\mathbf{f}_n}^{\top} = \mathbf{I}_{d_{\mathcal{Z}}}$ , then there exist orthogonal matrices  $\mathbf{Q}_n \in O(d_{\mathcal{Z}})$  such that

$$\mathbf{Q}_n \mathbf{U}_{\mathbf{f}_n}(\mathbf{f}_n - \boldsymbol{\mu}_n) \xrightarrow[n \rightarrow \infty]{L^2} \mathbf{W}_{\mathbf{f}}(\mathbf{f} - \boldsymbol{\mu}).$$

*Proof.*

**1. Convergence of moments.**

Since  $\mathbf{f}_n \rightarrow \mathbf{f}$  in  $L^2(P_{\mathbf{x}})$ , we have  $\|\mathbf{f}_n - \mathbf{f}\|_{L^2}^2 = \mathbb{E}[\|\mathbf{f}_n - \mathbf{f}\|^2] \rightarrow 0$ . By the Cauchy-Schwarz inequality,

$$\|\boldsymbol{\mu}_n - \boldsymbol{\mu}\| = \|\mathbb{E}[\mathbf{f}_n - \mathbf{f}]\| \leq \mathbb{E}[\|\mathbf{f}_n - \mathbf{f}\|] \leq \|\mathbf{f}_n - \mathbf{f}\|_{L^2} \longrightarrow 0.$$

For the second moment matrices, each entry of  $\mathbb{E}[\mathbf{f}_n \mathbf{f}_n^\top]$  converges to the corresponding entry of  $\mathbb{E}[\mathbf{f} \mathbf{f}^\top]$  because

$$\|\mathbf{f}_n \mathbf{f}_n^\top - \mathbf{f} \mathbf{f}^\top\|_F \leq (\|\mathbf{f}_n\| + \|\mathbf{f}\|) \|\mathbf{f}_n - \mathbf{f}\|,$$

and taking expectations yields

$$\|\mathbb{E}[\mathbf{f}_n \mathbf{f}_n^\top] - \mathbb{E}[\mathbf{f} \mathbf{f}^\top]\| \leq \mathbb{E}[\|\mathbf{f}_n \mathbf{f}_n^\top - \mathbf{f} \mathbf{f}^\top\|] \leq (\|\mathbf{f}_n\|_{L^2} + \|\mathbf{f}\|_{L^2}) \|\mathbf{f}_n - \mathbf{f}\|_{L^2} \rightarrow 0,$$

so  $\mathbb{E}[\mathbf{f}_n \mathbf{f}_n^\top] \rightarrow \mathbb{E}[\mathbf{f} \mathbf{f}^\top]$  in operator norm.

Combining the above,

$$\mathbf{\Sigma}_{\mathbf{f}_n} = \mathbb{E}[(\mathbf{f}_n - \boldsymbol{\mu}_n)(\mathbf{f}_n - \boldsymbol{\mu}_n)^\top] = \mathbb{E}[\mathbf{f}_n \mathbf{f}_n^\top] - \boldsymbol{\mu}_n \boldsymbol{\mu}_n^\top \xrightarrow[n \rightarrow \infty]{\|\cdot\|} \mathbb{E}[\mathbf{f} \mathbf{f}^\top] - \boldsymbol{\mu} \boldsymbol{\mu}^\top = \mathbf{\Sigma}_{\mathbf{f}}.$$

## 2. Positive definiteness and bounded whitening operators.

Since  $\mathbf{\Sigma}_{\mathbf{f}} \succ 0$ , all its eigenvalues are positive. Let  $\sigma_{\min} > 0$  denote its smallest eigenvalue, i.e.,

$$\sigma_{\min} := \sigma_{\min}(\mathbf{\Sigma}_{\mathbf{f}}) \quad \text{so that} \quad \mathbf{\Sigma}_{\mathbf{f}} \succeq \sigma_{\min} \mathbf{I}.$$

Because  $\mathbf{\Sigma}_{\mathbf{f}_n} \rightarrow \mathbf{\Sigma}_{\mathbf{f}}$  in operator norm, we have

$$\|\mathbf{\Sigma}_{\mathbf{f}_n} - \mathbf{\Sigma}_{\mathbf{f}}\| \xrightarrow[n \rightarrow \infty]{} 0.$$

By Weyl's eigenvalue perturbation inequality,

$$\forall i \in [1, \dots, d_{\mathcal{Z}}], \quad |\sigma_i(\mathbf{\Sigma}_{\mathbf{f}_n}) - \sigma_i(\mathbf{\Sigma}_{\mathbf{f}})| \leq \|\mathbf{\Sigma}_{\mathbf{f}_n} - \mathbf{\Sigma}_{\mathbf{f}}\|.$$

Hence for sufficiently large  $n$ ,

$$\sigma_{\min}(\mathbf{\Sigma}_{\mathbf{f}_n}) \geq \sigma_{\min}(\mathbf{\Sigma}_{\mathbf{f}}) - \|\mathbf{\Sigma}_{\mathbf{f}_n} - \mathbf{\Sigma}_{\mathbf{f}}\| \geq \frac{\sigma_{\min}}{2} > 0.$$

Therefore each  $\mathbf{\Sigma}_{\mathbf{f}_n}$  is symmetric positive definite and satisfies

$$\mathbf{\Sigma}_{\mathbf{f}_n} \succeq \frac{\sigma_{\min}}{2} \mathbf{I}.$$

Taking inverse square roots preserves the Löwner order on the SPD cone, so

$$\|\mathbf{W}_{\mathbf{f}_n}\| = \|\mathbf{\Sigma}_{\mathbf{f}_n}^{-1/2}\| = (\sigma_{\min}(\mathbf{\Sigma}_{\mathbf{f}_n}))^{-1/2} \leq (\sigma_{\min}/2)^{-1/2}.$$

Thus the sequence  $\{\mathbf{W}_{\mathbf{f}_n}\}$  is uniformly bounded in operator norm.

## 3. Continuity of matrix square roots.

Since  $\mathbf{\Sigma}_{\mathbf{f}} \succ 0$  and  $\mathbf{\Sigma}_{\mathbf{f}_n} \rightarrow \mathbf{\Sigma}_{\mathbf{f}}$  in operator norm, there exist constants

$$m := \frac{\sigma_{\min}(\mathbf{\Sigma}_{\mathbf{f}})}{2} > 0, \quad M := \|\mathbf{\Sigma}_{\mathbf{f}}\| + 1,$$

and an integer  $N$  such that for all  $n \geq N$ , the spectra satisfy  $\sigma(\mathbf{\Sigma}_{\mathbf{f}_n}), \sigma(\mathbf{\Sigma}_{\mathbf{f}}) \subset [m, M]$ .

Fix  $\varepsilon > 0$ . By the Weierstrass approximation theorem, there exists a polynomial  $p$  such that

$$\sup_{\sigma \in [m, M]} |\sigma^{-1/2} - p(\sigma)| < \varepsilon/3.$$

Using the continuous functional calculus for self-adjoint matrices, we have

$$\|\mathbf{\Sigma}_{\mathbf{f}_n}^{-1/2} - \mathbf{\Sigma}_{\mathbf{f}}^{-1/2}\| \leq \|\mathbf{\Sigma}_{\mathbf{f}_n}^{-1/2} - p(\mathbf{\Sigma}_{\mathbf{f}_n})\| + \|p(\mathbf{\Sigma}_{\mathbf{f}_n}) - p(\mathbf{\Sigma}_{\mathbf{f}})\| + \|p(\mathbf{\Sigma}_{\mathbf{f}}) - \mathbf{\Sigma}_{\mathbf{f}}^{-1/2}\|.$$

The first and third terms are each bounded by  $\sup_{\sigma \in [m, M]} |\sigma^{-1/2} - p(\sigma)| < \varepsilon/3$ . For the middle term, note that  $p(A) = \sum_k a_k A^k$  is a finite polynomial, hence norm-continuous; since  $\mathbf{\Sigma}_{\mathbf{f}_n} \rightarrow \mathbf{\Sigma}_{\mathbf{f}}$ , we have  $\|p(\mathbf{\Sigma}_{\mathbf{f}_n}) - p(\mathbf{\Sigma}_{\mathbf{f}})\| < \varepsilon/3$  for all large  $n$ . Therefore  $\|\mathbf{\Sigma}_{\mathbf{f}_n}^{-1/2} - \mathbf{\Sigma}_{\mathbf{f}}^{-1/2}\| < \varepsilon$  for  $n$  sufficiently large, i.e.

$$\mathbf{W}_{\mathbf{f}_n} = \mathbf{\Sigma}_{\mathbf{f}_n}^{-1/2} \xrightarrow[n \rightarrow \infty]{\|\cdot\|} \mathbf{\Sigma}_{\mathbf{f}}^{-1/2} = \mathbf{W}_{\mathbf{f}}.$$

---

#### 4. $L^2$ -continuity of whitening.

Define the difference

$$\mathbf{\Delta}_n := \mathbf{W}_{\mathbf{f}_n}(\mathbf{f}_n - \boldsymbol{\mu}_n) - \mathbf{W}_{\mathbf{f}}(\mathbf{f} - \boldsymbol{\mu}) = (\mathbf{W}_{\mathbf{f}_n} - \mathbf{W}_{\mathbf{f}})(\mathbf{f} - \boldsymbol{\mu}) + \mathbf{W}_{\mathbf{f}_n}[(\mathbf{f}_n - \boldsymbol{\mu}_n) - (\mathbf{f} - \boldsymbol{\mu})].$$

Taking  $L^2$  norms and applying Cauchy-Schwarz,

$$\|\mathbf{\Delta}_n\|_{L^2} \leq \|\mathbf{W}_{\mathbf{f}_n} - \mathbf{W}_{\mathbf{f}}\| \|\mathbf{f} - \boldsymbol{\mu}\|_{L^2} + \|\mathbf{W}_{\mathbf{f}_n}\| \|(\mathbf{f}_n - \boldsymbol{\mu}_n) - (\mathbf{f} - \boldsymbol{\mu})\|_{L^2}.$$

The first term tends to 0 because  $\mathbf{W}_{\mathbf{f}_n} \rightarrow \mathbf{W}_{\mathbf{f}}$  and  $\|\mathbf{f} - \boldsymbol{\mu}\|_{L^2} < \infty$ . For the second term,  $\|\mathbf{W}_{\mathbf{f}_n}\|$  is uniformly bounded and

$$\|(\mathbf{f}_n - \boldsymbol{\mu}_n) - (\mathbf{f} - \boldsymbol{\mu})\|_{L^2} \leq \|\mathbf{f}_n - \mathbf{f}\|_{L^2} + \|\boldsymbol{\mu}_n - \boldsymbol{\mu}\| \rightarrow 0.$$

Thus  $\|\mathbf{\Delta}_n\|_{L^2} \rightarrow 0$ , proving Equation 14.

#### 5. Orthogonal alignment for general whiteners.

Let  $\mathbf{U}_{\mathbf{f}_n} \in \text{GL}(d_{\mathcal{Z}})$  satisfy  $\mathbf{U}_{\mathbf{f}_n} \boldsymbol{\Sigma}_{\mathbf{f}_n} \mathbf{U}_{\mathbf{f}_n}^\top = \mathbf{I}_{d_{\mathcal{Z}}}$ . Using the polar decomposition,

$$\mathbf{U}_{\mathbf{f}_n} \boldsymbol{\Sigma}_{\mathbf{f}_n}^{1/2} = \mathbf{Q}_n, \quad \mathbf{Q}_n \in O(d_{\mathcal{Z}}),$$

which implies  $\mathbf{Q}_n \mathbf{U}_{\mathbf{f}_n} = \boldsymbol{\Sigma}_{\mathbf{f}_n}^{-1/2} = \mathbf{W}_{\mathbf{f}_n}$ . Therefore,

$$\mathbf{Q}_n \mathbf{U}_{\mathbf{f}_n}(\mathbf{f}_n - \boldsymbol{\mu}_n) = \mathbf{W}_{\mathbf{f}_n}(\mathbf{f}_n - \boldsymbol{\mu}_n) \xrightarrow[n \rightarrow \infty]{L^2} \mathbf{W}_{\mathbf{f}}(\mathbf{f} - \boldsymbol{\mu})$$

by the first part, completing the proof.  $\square$

**Lemma 6** (Reparameterization Invariance and Representational Universality of CCA). *Let  $\mathcal{S}, \mathcal{X}, \mathcal{X}'$  be standard Borel spaces and  $\mathbf{g}, \mathbf{g}'$  be Borel-measurable and injective. In addition, let  $\tilde{\mathcal{F}}_{\mathcal{X}}, \tilde{\mathcal{F}}_{\mathcal{X}'}$  be the whitened encoder classes of Definition 2 and assume that the base encoders  $\mathbf{f}, \mathbf{f}'$  underlying  $\tilde{\mathcal{F}}_{\mathcal{X}}, \tilde{\mathcal{F}}_{\mathcal{X}'}$  are dense in  $L^2(P_{\mathbf{x}}; \mathbb{R}^{d_{\mathcal{Z}}})$  and  $L^2(P_{\mathbf{x}'}; \mathbb{R}^{d_{\mathcal{Z}}})$ , respectively. Define whitened representable latent classes:*

$$\tilde{\mathcal{F}}_{\mathcal{S}} := \{\tilde{\mathbf{f}} \circ \mathbf{g} : \tilde{\mathbf{f}} \in \tilde{\mathcal{F}}_{\mathcal{X}}\}, \quad \tilde{\mathcal{F}}'_{\mathcal{S}} := \{\tilde{\mathbf{f}}' \circ \mathbf{g}' : \tilde{\mathbf{f}}' \in \tilde{\mathcal{F}}'_{\mathcal{X}'}\},$$

and the whitened feasible latent classes:

$$\begin{aligned} \hat{\mathcal{F}}_{\mathcal{S}} &:= \{\hat{\mathbf{h}} \in L^2(P_{\mathbf{s}}; d_{\mathcal{Z}}) : \mathbb{E}[\hat{\mathbf{h}}(\mathbf{s})] = 0, \text{Cov}(\hat{\mathbf{h}}(\mathbf{s})) = \mathbf{I}_{d_{\mathcal{Z}}}\}, \\ \hat{\mathcal{F}}'_{\mathcal{S}} &:= \{\hat{\mathbf{h}} \in L^2(P_{\mathbf{s}'}; d_{\mathcal{Z}}) : \mathbb{E}[\hat{\mathbf{h}}(\mathbf{s}')] = 0, \text{Cov}(\hat{\mathbf{h}}(\mathbf{s}')) = \mathbf{I}_{d_{\mathcal{Z}}}\}. \end{aligned}$$

Further define the population CCA objective with respect to whitened feasible latent classes  $\hat{\mathcal{F}}_{\mathcal{S}}, \hat{\mathcal{F}}'_{\mathcal{S}}$  on their domains  $\mathcal{S} \times \mathcal{S}$ :

$$J_{\mathcal{S}}(\hat{\mathbf{h}}, \hat{\mathbf{h}}') = \sum_{i=1}^{d_{\mathcal{Z}}} \sigma_i(\text{Cov}(\hat{\mathbf{h}}(\mathbf{s}), \hat{\mathbf{h}}'(\mathbf{s}'))), \quad (15)$$

where  $\sigma_i(\cdot)$  denotes the  $i$ -th singular value. Then the following properties hold.

1. **Objective Preservation.**  $\forall(\tilde{\mathbf{f}}, \tilde{\mathbf{f}}') \in \tilde{\mathcal{F}}_{\mathcal{X}} \times \tilde{\mathcal{F}}'_{\mathcal{X}'}, J(\tilde{\mathbf{f}}, \tilde{\mathbf{f}}') = J_{\mathcal{S}}(\tilde{\mathbf{f}} \circ \mathbf{g}, \tilde{\mathbf{f}}' \circ \mathbf{g}')$ .
2. **Maximizer Correspondence.** If  $(\tilde{\mathbf{f}}^*, \tilde{\mathbf{f}}'^*)$  is a maximizer of  $J$  in ?? over  $\tilde{\mathcal{F}}_{\mathcal{X}} \times \tilde{\mathcal{F}}'_{\mathcal{X}'}$ , then its composition  $(\tilde{\mathbf{f}}^* \circ \mathbf{g}, \tilde{\mathbf{f}}'^* \circ \mathbf{g}')$  is also a maximizer of  $J_{\mathcal{S}}$  in Equation 15 over  $\tilde{\mathcal{F}}_{\mathcal{S}} \times \tilde{\mathcal{F}}'_{\mathcal{S}}$ , and conversely.
3. **Representation Universality.** For any  $\hat{\mathbf{h}} \in \hat{\mathcal{F}}_{\mathcal{S}}, \hat{\mathbf{h}}' \in \hat{\mathcal{F}}'_{\mathcal{S}}$ , and any  $\epsilon, \epsilon' > 0$ , there exist  $\tilde{\mathbf{h}} \in \tilde{\mathcal{F}}_{\mathcal{S}}$  and  $\tilde{\mathbf{h}}' \in \tilde{\mathcal{F}}'_{\mathcal{S}}$  such that

$$\mathbb{E}[\|\hat{\mathbf{h}}(\mathbf{s}) - \tilde{\mathbf{h}}(\mathbf{s})\|^2] < \epsilon^2 \quad \text{and} \quad \mathbb{E}[\|\hat{\mathbf{h}}'(\mathbf{s}') - \tilde{\mathbf{h}}'(\mathbf{s}')\|^2] < \epsilon'^2.$$

*Proof.* We work in  $L^2$ , identifying functions that agree  $P$ -a.s. Let  $J$  be the CCA objective on  $\mathcal{X} \times \mathcal{X}'$  from ?? and  $J_S$  the latent CCA objective on  $\mathcal{S} \times \mathcal{S}'$  from Equation 15.

### 1. Objective preservation.

By the whitening preservation of Lemma 3.3, the two cross-covariance matrices  $\text{Cov}(\tilde{\mathbf{f}}, \tilde{\mathbf{f}}')$ ,  $\text{Cov}(\tilde{\mathbf{f}} \circ \mathbf{g}, \tilde{\mathbf{f}}' \circ \mathbf{g}')$  coincide, hence so do their sum of the singular values:

$$J(\tilde{\mathbf{f}}, \tilde{\mathbf{f}}') = J_S(\tilde{\mathbf{f}} \circ \mathbf{g}, \tilde{\mathbf{f}}' \circ \mathbf{g}').$$

### 2. Maximizer correspondence (between representable classes).

Since the composition map

$$\Psi : \tilde{\mathcal{F}}_{\mathcal{X}} \times \tilde{\mathcal{F}}'_{\mathcal{X}'} \rightarrow \tilde{\mathcal{F}}_{\mathcal{S}} \times \tilde{\mathcal{F}}'_{\mathcal{S}'}, \quad \Psi(\tilde{\mathbf{f}}, \tilde{\mathbf{f}}') = (\tilde{\mathbf{f}} \circ \mathbf{g}, \tilde{\mathbf{f}}' \circ \mathbf{g}').$$

is bijective, given by Lemma 4.2, and the objective preservation in Lemma 6.1 implies

$$\Phi \left( \underset{\tilde{\mathcal{F}}_{\mathcal{X}} \times \tilde{\mathcal{F}}'_{\mathcal{X}'}}{\text{argmax}} J \right) = \underset{\tilde{\mathcal{F}}_{\mathcal{S}} \times \tilde{\mathcal{F}}'_{\mathcal{S}'}}{\text{argmax}} J_S.$$

If  $(\tilde{\mathbf{f}}^*, \tilde{\mathbf{f}}'^*)$  is a maximizer on  $\tilde{\mathcal{F}}_{\mathcal{X}} \times \tilde{\mathcal{F}}'_{\mathcal{X}'}$ , then  $(\tilde{\mathbf{f}}^* \circ \mathbf{g}, \tilde{\mathbf{f}}'^* \circ \mathbf{g}')$  is also a maximizer on  $\tilde{\mathcal{F}}_{\mathcal{S}} \times \tilde{\mathcal{F}}'_{\mathcal{S}'}$ , and conversely.

### 3. Representation Universality.

Fix  $\hat{\mathbf{h}} \in \hat{\mathcal{F}}_{\mathcal{S}}$  and  $\epsilon > 0$ . We show there exists  $\tilde{\mathbf{h}} \in \tilde{\mathcal{F}}_{\mathcal{S}}$  with  $\mathbb{E}[\|\hat{\mathbf{h}}(\mathbf{s}) - \tilde{\mathbf{h}}(\mathbf{s})\|^2] < \epsilon^2$ . (The primed side is identical.)

(i) *Pull back  $\hat{\mathbf{h}}$  to the observation domain.* By Lemma 4.2 (measurable inverses on images), the Borel inverse  $\mathbf{g}^{-1} : \mathbf{g}(\mathcal{S}) \rightarrow \mathcal{S}$  exists. Define on  $\mathbf{g}(\mathcal{S})$

$$\hat{\mathbf{h}}_{\mathcal{X}} := \hat{\mathbf{h}} \circ \mathbf{g}^{-1},$$

and extend it arbitrarily to a Borel function on  $\mathcal{X}$  (the extension does not affect  $L^2(P_{\mathbf{x}})$  since  $P_{\mathbf{x}}$  is supported on  $\mathbf{g}(\mathcal{S})$ ). By Lemma 3.2-3 (expectation/covariance preservation and whitening preservation),  $\hat{\mathbf{h}} \in \hat{\mathcal{F}}_{\mathcal{S}}$  implies

$$\hat{\mathbf{h}}_{\mathcal{X}} \in \hat{\mathcal{F}}_{\mathcal{X}} := \{ \mathbf{u} \in L^2(P_{\mathbf{x}}; \mathbb{R}^{d_z}) : \mathbb{E}[\mathbf{u}(\mathbf{x})] = \mathbf{0}, \text{Cov}(\mathbf{u}(\mathbf{x})) = \mathbf{I} \}.$$

(ii) *Approximate in  $L^2(P_{\mathbf{x}})$  by base encoders.* By the density assumption in Definition 2, there exists a sequence  $\{\mathbf{f}_n\}_{n \geq 1} \subset \mathcal{H}_{\mathcal{X}}$  such that

$$\|\mathbf{f}_n - \hat{\mathbf{h}}_{\mathcal{X}}\|_{L^2(P_{\mathbf{x}})} \xrightarrow{n \rightarrow \infty} 0.$$

Write  $\boldsymbol{\mu}_n = \mathbb{E}[\mathbf{f}_n(\mathbf{x})]$  and  $\boldsymbol{\Sigma}_{\mathbf{f}_n} = \text{Cov}(\mathbf{f}_n(\mathbf{x}))$ . Since  $\hat{\mathbf{h}}_{\mathcal{X}} \in L^2$  and  $\mathbf{f}_n \rightarrow \hat{\mathbf{h}}_{\mathcal{X}}$  in  $L^2$ , Lemma 5.1 implies  $\boldsymbol{\mu}_n \rightarrow \mathbf{0}$  and  $\boldsymbol{\Sigma}_{\mathbf{f}_n} \rightarrow \mathbf{I}$  in operator norm; in particular,  $\boldsymbol{\Sigma}_{\mathbf{f}_n} \succ 0$  for all large  $n$ .

(iii) *Whiten the approximants and pass limits through whitening.* Let  $\mathbf{W}_{\mathbf{f}_n} = \boldsymbol{\Sigma}_{\mathbf{f}_n}^{-1/2}$  and define the whitened encoders

$$\tilde{\mathbf{f}}_n := \mathbf{W}_{\mathbf{f}_n} (\mathbf{f}_n - \boldsymbol{\mu}_n) \in \tilde{\mathcal{F}}_{\mathcal{X}}.$$

By Lemma 5.4,

$$\tilde{\mathbf{f}}_n \xrightarrow[n \rightarrow \infty]{L^2(P_{\mathbf{x}})} \boldsymbol{\Sigma}_{\hat{\mathbf{h}}_{\mathcal{X}}}^{-1/2} (\hat{\mathbf{h}}_{\mathcal{X}} - \mathbb{E}[\hat{\mathbf{h}}_{\mathcal{X}}]) = \hat{\mathbf{h}}_{\mathcal{X}},$$

since  $\hat{\mathbf{h}}_{\mathcal{X}}$  is already whitened (mean 0, covariance  $\mathbf{I}$ ). Hence there exists  $N$  such that  $\|\tilde{\mathbf{f}}_N - \hat{\mathbf{h}}_{\mathcal{X}}\|_{L^2(P_{\mathbf{x}})} < \epsilon$ .

(iv) *Push forward to the latent domain and conclude.* Set  $\tilde{\mathbf{h}} := \tilde{\mathbf{f}}_N \circ \mathbf{g} \in \tilde{\mathcal{F}}_{\mathcal{S}}$  by definition of the representable class. By Lemma 4.1 (composition isometry),

$$\|\tilde{\mathbf{h}} - \hat{\mathbf{h}}\|_{L^2(P_{\mathbf{s}})} = \|\tilde{\mathbf{f}}_N \circ \mathbf{g} - \hat{\mathbf{h}}_{\mathcal{X}} \circ \mathbf{g}\|_{L^2(P_{\mathbf{s}})} = \|\tilde{\mathbf{f}}_N - \hat{\mathbf{h}}_{\mathcal{X}}\|_{L^2(P_{\mathbf{x}})} < \epsilon.$$

Therefore  $\mathbb{E}[\|\hat{\mathbf{h}}(\mathbf{s}) - \tilde{\mathbf{h}}(\mathbf{s})\|^2] < \epsilon^2$ . Since  $\epsilon > 0$  was arbitrary, the claim follows. The proof on the primed side is identical, yielding  $\tilde{\mathbf{h}}' \in \tilde{\mathcal{F}}'_{\mathcal{S}'}$  with  $\mathbb{E}[\|\hat{\mathbf{h}}'(\mathbf{s}') - \tilde{\mathbf{h}}'(\mathbf{s}')\|^2] < \epsilon'^2$  for any  $\epsilon' > 0$ .

□

## 8.2 Normalized Hermite-Mehler expansion of joint Gaussian distribution

**Lemma 7** (Hermite-Mehler expansion of bivariate Gaussian density). *Let  $s, s'$  be jointly Gaussian with means  $\mu_S, \mu_{S'}$ , variances  $\sigma_s^2, \sigma_{s'}^2$ , and correlation coefficient  $t$  with  $|t| < 1$ . Set*

$$x = \frac{s - \mu_S}{\sigma_s}, \quad y = \frac{s' - \mu_{S'}}{\sigma_{s'}}, \quad u = \frac{x}{\sqrt{2}}, \quad v = \frac{y}{\sqrt{2}}.$$

Let  $H_n$  denote the physicists' Hermite polynomials and define the normalized Hermite polynomials as

$$\psi_n(z) = \frac{1}{\sqrt{2^n n!} \sqrt{\pi}} H_n(z).$$

Then the joint density  $\phi(s, s')$  admits the Hermite-Mehler expansions

$$P_{SS}(s, s') = \frac{1}{2\sigma_s \sigma_{s'}} P_{UV}(u, v) = \frac{1}{\sigma_s \sigma_{s'}} P_{XY}(x, y) = \frac{1}{2\pi \sigma_s \sigma_{s'}} e^{-(u^2+v^2)} \sum_{n=0}^{\infty} \frac{t^n}{2^n n!} H_n(u) H_n(v) \quad (16)$$

$$= \frac{1}{2\sqrt{\pi} \sigma_s \sigma_{s'}} e^{-(u^2+v^2)} \sum_{n=0}^{\infty} t^n \psi_n(u) \psi_n(v). \quad (17)$$

The series converge absolutely for  $|t| < 1$ .

*Proof.* Mehler's formula for physicists' Hermite polynomials states that for  $|t| < 1$ ,

$$\sum_{n=0}^{\infty} \frac{t^n}{2^n n!} H_n(u) H_n(v) = \frac{1}{\sqrt{1-t^2}} \exp\left(\frac{2tuv - t^2(u^2 + v^2)}{1-t^2}\right).$$

Multiply both sides by  $\frac{1}{2\pi \sigma_s \sigma_{s'} \sigma_x \sigma_y} e^{-(u^2+v^2)}$ . On the right,

$$\frac{1}{2\pi \sigma_s \sigma_{s'} \sigma_x \sigma_y} \frac{1}{\sqrt{1-t^2}} \exp\left(- (u^2 + v^2) + \frac{2tuv - t^2(u^2 + v^2)}{1-t^2}\right) = \frac{1}{2\pi \sigma_s \sigma_{s'} \sigma_x \sigma_y \sqrt{1-t^2}} \exp\left(-\frac{(u^2 - 2tuv + v^2)}{1-t^2}\right).$$

Plug in  $u = x/\sqrt{2}$  and  $v = y/\sqrt{2}$ , the exponent becomes

$$-\frac{x^2 - 2txy + y^2}{2(1-t^2)},$$

and the RHS becomes

$$\frac{1}{2\pi \sigma_s \sigma_{s'} \sigma_x \sigma_y \sqrt{1-t^2}} \exp\left(-\frac{x^2 - 2txy + y^2}{2(1-t^2)}\right).$$

Since the density of bivariate Gaussian distribution of  $(x, y)$  is:

$$P_{XY}(x, y) = \frac{1}{2\pi \sigma_x \sigma_y \sqrt{1-t^2}} \exp\left(-\frac{x^2 - 2txy + y^2}{2(1-t^2)}\right),$$

hence the correlation of between  $(u, v)$  is equal to  $x, y$ , then

$$P_{SS}(s, s') = \frac{1}{\sigma_s \sigma_{s'}} \phi_{XY}(x, y) = \frac{1}{2\pi \sigma_s \sigma_{s'} \sigma_x \sigma_y} e^{-(u^2+v^2)} \sum_{n=0}^{\infty} \frac{t^n}{2^n n!} H_n(u) H_n(v),$$

given  $\sigma_x = \sigma_y = 1$  (standardization by change of variable), we have

$$P_{SS}(s, s') = \frac{1}{\sigma_s \sigma_{s'}} P_{XY}(x, y) = \frac{1}{2\pi \sigma_s \sigma_{s'}} e^{-(u^2+v^2)} \sum_{n=0}^{\infty} \frac{t^n}{2^n n!} H_n(u) H_n(v).$$

Equating with the left-hand side yields the first equality in Equation 16. The second equality follows by substituting  $H_n(z) = \sqrt{2^n n!} \sqrt{\pi} \psi_n(z)$  and simplifying:

$$P_{SS}(s, s') = \frac{1}{2\sigma_s \sigma_{s'}} P_{UV}(u, v) = \frac{1}{2\pi \sigma_s \sigma_{s'}} e^{-(u^2+v^2)} \sum_{n=0}^{\infty} \frac{t^n}{2^n n!} H_n(u) H_n(v) = \frac{1}{2\sigma_s \sigma_{s'}} e^{-(u^2+v^2)} \sum_{n=0}^{\infty} t^n \psi_n(u) \psi_n(v).$$

□

*Remark.* The functions  $\{\psi_n\}_{n \geq 0}$  are orthonormal in  $L^2(\mathbb{R}, e^{-z^2} dz)$ , i.e.,  $\int_{\mathbb{R}} \psi_m(z) \psi_n(z) e^{-z^2} dz = \delta_{mn}$ . Writing the density in the second form of Equation 16 cleanly separates the Gaussian weight  $e^{-(u^2+v^2)}$  from the orthonormal basis functions.

**Proposition 1** (Hermite-Mehler expansion of joint Gaussian distribution). *Let  $\mathbf{s} = (s_1, \dots, s_{d_S})$  and  $\mathbf{s}' = (s'_1, \dots, s'_{d_S})$  be  $d_S$ -dimensional jointly Gaussian random vectors. Assume that the coordinate pairs  $(s_i, s'_i)$  are mutually independent across  $i = 1, \dots, d_S$ , with each pair being bivariate Gaussian with means  $\mu_{s_i}, \mu_{s'_i}$ , variances  $\sigma_{s_i}^2, \sigma_{s'_i}^2$ , and correlation coefficient  $t_i$  satisfying  $|t_i| < 1$ .*

Define the normalized multivariate Hermite polynomials

$$\Psi_{\mathbf{n}}(\mathbf{x}) = \prod_{i=1}^{d_S} \psi_{n_i}(x_i), \quad \mathbf{n} = (n_1, \dots, n_{d_S}) \in \mathbb{N}^{d_S}.$$

Then the joint density of  $(\mathbf{s}, \mathbf{s}')$  admits the expansion

$$\phi(\mathbf{s}, \mathbf{s}') = c \cdot e^{-(\|\mathbf{u}\|^2 + \|\mathbf{v}\|^2)} \sum_{\mathbf{n} \in \mathbb{N}^{d_S}} t_{\mathbf{n}} \Psi_{\mathbf{n}}(\mathbf{u}) \Psi_{\mathbf{n}}(\mathbf{v}), \quad (18)$$

where

$$c = \left( \frac{1}{2\sqrt{\pi}} \right)^{d_S} \prod_{i=1}^{d_S} \frac{1}{\sigma_{s_i} \sigma_{s'_i}}, \quad t_{\mathbf{n}} = \prod_{j=1}^{d_S} t_j^{n_j},$$

and

$$u_i = \frac{s_i - \mu_{s_i}}{\sqrt{2} \sigma_{s_i}}, \quad v_i = \frac{s'_i - \mu_{s'_i}}{\sqrt{2} \sigma_{s'_i}}, \quad i = 1, \dots, d_S.$$

*Proof.* We now consider  $d_S$ -dimensional Gaussian vectors  $\mathbf{s} = (s_1, \dots, s_{d_S})$  and  $\mathbf{s}' = (s'_1, \dots, s'_{d_S})$ . Under ??,  $\forall i \in [1, \dots, d_S]$  the pairs  $(s_i, s'_i)$  of ground-truth latent pair can be transformed to be mutually independent via whitening. Here, we assume that  $(s_i, s'_i)$ ,  $\forall i \in [1, \dots, d_S]$  are already mutually independent, so the joint density factorizes as

$$P_{SS}(\mathbf{s}, \mathbf{s}') = \prod_{i=1}^{d_S} \phi(s_i, s'_i).$$

Substituting Equation 16 for each factor yields

$$P_{SS}(\mathbf{s}, \mathbf{s}') = \left( \frac{1}{2\sqrt{\pi}} \right)^{d_S} \prod_{i=1}^{d_S} \frac{1}{\sigma_{s_i} \sigma_{s'_i}} \prod_{j=1}^{d_S} e^{-(u_j^2 + v_j^2)} \prod_{k=1}^{d_S} \left[ \sum_{n=0}^{\infty} t_k^n \psi_n(u_k) \psi_n(v_k) \right].$$

Expanding the product of sums gives a series indexed by multi-indices  $\mathbf{n} = (n_1, \dots, n_{d_S}) \in \mathbb{N}^{d_S}$ :

$$P_{SS}(\mathbf{s}, \mathbf{s}') = \left( \frac{1}{2\sqrt{\pi}} \right)^{d_S} \prod_{i=1}^{d_S} \frac{1}{\sigma_{s_i} \sigma_{s'_i}} \prod_{j=1}^{d_S} e^{-(u_j^2 + v_j^2)} \sum_{\mathbf{n} \in \mathbb{N}^{d_S}} \left[ \prod_{j=1}^{d_S} t_j^{n_j} \psi_{n_j}(u_j) \psi_{n_j}(v_j) \right].$$

Introducing the tensor-product Hermite basis (multi-variant normalized Hermite polynomials)

$$\Psi_{\mathbf{n}}(\mathbf{x}) = \prod_{i=1}^{d_S} \psi_{n_i}(x_i), \quad \mathbf{x} = (x_1, \dots, x_{d_S}) \in \mathbb{R}^{d_S},$$

the expansion can be written compactly as

$$P_{SS}(\mathbf{s}, \mathbf{s}') = c \cdot e^{-(\|\mathbf{u}\|^2 + \|\mathbf{v}\|^2)} \sum_{\mathbf{n} \in \mathbb{N}^{d_S}} t_{\mathbf{n}} \Psi_{\mathbf{n}}(\mathbf{u}) \Psi_{\mathbf{n}}(\mathbf{v}),$$

where

$$c = \left( \frac{1}{2\sqrt{\pi}} \right)^{d_S} \prod_{i=1}^{d_S} \frac{1}{\sigma_{s_i} \sigma_{s'_i}}, \quad t_{\mathbf{n}} = \prod_{j=1}^{d_S} t_j^{n_j}, \quad (19)$$

and

$$u_i = \frac{s_i - \mu_{s_i}}{\sqrt{2} \sigma_{s_i}}, \quad v_i = \frac{s'_i - \mu_{s'_i}}{\sqrt{2} \sigma_{s'_i}}, \quad i = 1, \dots, d_S.$$

For a comprehensive introduction to multi-variate Hermite polynomials, refer to Section 2.5.3 of Dunkl and Xu [2014].  $\square$

## 9 Proof of Lemma 2

*Proof of Lemma 2.* Fix a pair  $(i, j)$  and write  $r := r_{ij}$  and  $t_k := t_{ij,k} \in [0, 1)$  for  $k = 1, \dots, r$ . By Lemma 1, the cross-view coupling term equals a product of  $r$  independent bivariate standard-normal densities:

$$\mathcal{K}_{ij}(\mathbf{u}, \mathbf{v}) = \prod_{k=1}^r \phi_{t_k}(u_k, v_k), \quad \mathbf{u}, \mathbf{v} \in \mathbb{R}^r, \quad (20)$$

where  $\phi(\cdot)$  is the univariate standard normal density and  $\phi_t(\cdot, \cdot)$  is the bivariate standard normal density with correlation  $t$ .

**Step 1: Bivariate Mehler–Hermite expansion normalized for  $\phi$ .** Let  $(X, Y)$  be bivariate standard normal with correlation  $t \in (-1, 1)$ . Lemma 7 in the appendix, specialized to  $\mu_S = \mu_{S'} = 0$  and  $\sigma_s = \sigma_{s'} = 1$ , gives

$$\phi_t(X, Y) = \frac{1}{2\sqrt{\pi}} e^{-(X^2+Y^2)/2} \sum_{n=0}^{\infty} t^n \psi_n^{(\text{app})}\left(\frac{X}{\sqrt{2}}\right) \psi_n^{(\text{app})}\left(\frac{Y}{\sqrt{2}}\right), \quad (21)$$

where (in the appendix normalization)

$$\psi_n^{(\text{app})}(z) = \frac{1}{\sqrt{2^n n! \sqrt{\pi}}} H_n(z),$$

and  $\{\psi_n^{(\text{app})}\}_{n \geq 0}$  is orthonormal in  $L^2(\mathbb{R}, e^{-z^2} dz)$ .

To match the standard-normal weight  $\phi(x) = (2\pi)^{-1/2} e^{-x^2/2}$  used in this paper, define the rescaled (still physicists-form) normalized Hermite basis

$$\psi_n(x) := \pi^{1/4} \psi_n^{(\text{app})}\left(\frac{x}{\sqrt{2}}\right) = \frac{1}{\sqrt{2^n n!}} H_n\left(\frac{x}{\sqrt{2}}\right). \quad (22)$$

Then  $\psi_n^{(\text{app})}(x/\sqrt{2}) = \psi_n(x)/\pi^{1/4}$ , and substituting this into Equation 21 yields

$$\begin{aligned} \phi_t(X, Y) &= \frac{1}{2\sqrt{\pi}} e^{-(X^2+Y^2)/2} \sum_{n=0}^{\infty} t^n \frac{\psi_n(X)}{\pi^{1/4}} \frac{\psi_n(Y)}{\pi^{1/4}} \\ &= \frac{1}{2\pi} e^{-(X^2+Y^2)/2} \sum_{n=0}^{\infty} t^n \psi_n(X) \psi_n(Y) \\ &= \phi(X) \phi(Y) \sum_{n=0}^{\infty} t^n \psi_n(X) \psi_n(Y). \end{aligned} \quad (23)$$

Moreover, by the change of variables  $z = x/\sqrt{2}$  and the orthonormality of  $\{\psi_n^{(\text{app})}\}$  under  $e^{-z^2} dz$ , the rescaled basis Equation 22 satisfies

$$\int_{\mathbb{R}} \phi(x) \psi_m(x) \psi_n(x) dx = \delta_{mn}. \quad (24)$$

(Indeed,  $\phi(x) dx = (\pi^{-1/2}) e^{-x^2/2} dx$  under  $x = \sqrt{2} z$ .)

**Step 2: Tensorization over  $k = 1, \dots, r$ .** Apply Equation 23 to each factor  $\phi_{t_k}(u_k, v_k)$  in Equation 20:

$$\phi_{t_k}(u_k, v_k) = \phi(u_k)\phi(v_k) \sum_{n_k=0}^{\infty} t_k^{n_k} \psi_{n_k}(u_k)\psi_{n_k}(v_k).$$

Multiplying over  $k = 1, \dots, r$  gives

$$\mathcal{K}_{ij}(\mathbf{u}, \mathbf{v}) = \phi(\mathbf{u})\phi(\mathbf{v}) \prod_{k=1}^r \left( \sum_{n_k=0}^{\infty} t_k^{n_k} \psi_{n_k}(u_k)\psi_{n_k}(v_k) \right),$$

where  $\phi(\mathbf{u}) = \prod_{k=1}^r \phi(u_k)$  and similarly for  $\phi(\mathbf{v})$ . Each univariate series is absolutely convergent for  $|t_k| < 1$  (Lemma 7), and  $r < \infty$ , hence the multi-index series obtained by expanding this finite product is absolutely convergent:

$$\sum_{\mathbf{n} \in \mathbb{N}^r} \left| \prod_{k=1}^r t_k^{n_k} \psi_{n_k}(u_k)\psi_{n_k}(v_k) \right| = \prod_{k=1}^r \left( \sum_{n_k=0}^{\infty} |t_k|^{n_k} |\psi_{n_k}(u_k)\psi_{n_k}(v_k)| \right) < \infty.$$

Therefore we may expand the product and rearrange terms (Tonelli/Fubini), yielding

$$\mathcal{K}_{ij}(\mathbf{u}, \mathbf{v}) = \phi(\mathbf{u})\phi(\mathbf{v}) \sum_{\mathbf{n} \in \mathbb{N}^r} \left( \prod_{k=1}^r t_k^{n_k} \right) \left( \prod_{k=1}^r \psi_{n_k}(u_k) \right) \left( \prod_{k=1}^r \psi_{n_k}(v_k) \right).$$

Recognizing

$$t_{\mathbf{n}} := \prod_{k=1}^r t_k^{n_k}, \quad \Psi_{\mathbf{n}}(\mathbf{u}) := \prod_{k=1}^r \psi_{n_k}(u_k),$$

gives the desired expansion

$$\mathcal{K}_{ij}(\mathbf{u}, \mathbf{v}) = \phi(\mathbf{u})\phi(\mathbf{v}) \sum_{\mathbf{n} \in \mathbb{N}^r} t_{\mathbf{n}} \Psi_{\mathbf{n}}(\mathbf{u}) \Psi_{\mathbf{n}}(\mathbf{v}).$$

**Step 3: Orthonormality of the multivariate basis.** Using Equation 24 and Fubini's theorem, for any  $\mathbf{m}, \mathbf{n} \in \mathbb{N}^r$ ,

$$\int_{\mathbb{R}^r} \phi(\mathbf{u}) \Psi_{\mathbf{n}}(\mathbf{u}) \Psi_{\mathbf{m}}(\mathbf{u}) d\mathbf{u} = \prod_{k=1}^r \int_{\mathbb{R}} \phi(u_k) \psi_{n_k}(u_k) \psi_{m_k}(u_k) du_k = \prod_{k=1}^r \delta_{n_k m_k} = \delta_{\mathbf{nm}}.$$

This completes the proof.  $\square$

## 10 Proof of Theorem 5.1

*Proof of Theorem 5.1.* Fix a pair of distinct views  $i \neq j$  and write  $r := r_{ij} = \text{rank}(\mathbf{A}_i \mathbf{A}_j^T)$ . Throughout the proof we work at the population level and assume  $d_{\mathcal{Z}} \rightarrow \infty$ .

**Step 1: Reduce the problem to the source domain.** Let  $\tilde{\mathbf{h}}_{\ell} := \tilde{\mathbf{f}}_{\ell} \circ \mathbf{g}_{\ell}$  for  $\ell \in \{i, j\}$ . By reparameterization invariance (cf. Lemma 6), for any encoders  $\tilde{\mathbf{f}}_i, \tilde{\mathbf{f}}_j$  we have

$$\text{Cov}(\tilde{\mathbf{f}}_i(\mathbf{x}_i), \tilde{\mathbf{f}}_j(\mathbf{x}_j)) = \text{Cov}(\tilde{\mathbf{h}}_i(\mathbf{s}_i), \tilde{\mathbf{h}}_j(\mathbf{s}_j)), \quad \text{Cov}(\tilde{\mathbf{f}}_{\ell}(\mathbf{x}_{\ell})) = \text{Cov}(\tilde{\mathbf{h}}_{\ell}(\mathbf{s}_{\ell})),$$

and therefore optimizing the two-view term of Equation 2 over  $(\tilde{\mathbf{f}}_i, \tilde{\mathbf{f}}_j)$  is equivalent to optimizing it over  $(\tilde{\mathbf{h}}_i, \tilde{\mathbf{h}}_j)$ . Since  $(\tilde{\mathbf{f}}_i^*, \tilde{\mathbf{f}}_j^*)$  is a *whitened* population maximizer, its source-domain counterpart  $(\tilde{\mathbf{h}}_i^*, \tilde{\mathbf{h}}_j^*)$  satisfies

$$\mathbb{E}[\tilde{\mathbf{h}}_{\ell}^*(\mathbf{s}_{\ell})] = \mathbf{0}, \quad \text{Cov}(\tilde{\mathbf{h}}_{\ell}^*(\mathbf{s}_{\ell})) = \mathbf{I}, \quad \ell \in \{i, j\}.$$

Thus the two-view population objective reduces to

$$J_{ij}(\tilde{\mathbf{h}}_i, \tilde{\mathbf{h}}_j) := \|\text{Cov}(\tilde{\mathbf{h}}_i(\mathbf{s}_i), \tilde{\mathbf{h}}_j(\mathbf{s}_j))\|_*.$$

**Step 2: Canonical coordinates for the sources.** Under Assumption 1 (Gaussian case), each  $(\mathbf{s}_i, \mathbf{s}_j)$  is jointly Gaussian. Let

$$\mathbf{W}_i := \text{Cov}(\mathbf{s}_i)^{-1/2} = (\mathbf{A}_i \mathbf{A}_i^\top + \mathbf{I})^{-1/2}, \quad \mathbf{W}_j := \text{Cov}(\mathbf{s}_j)^{-1/2}.$$

Define the normalized cross-covariance (cf. Equation 5)

$$\mathbf{R}_{ij} := \text{Cov}(\mathbf{W}_i \mathbf{s}_i, \mathbf{W}_j \mathbf{s}_j) = \mathbf{W}_i \mathbf{A}_i \mathbf{A}_j^\top \mathbf{W}_j^\top,$$

and take an SVD  $\mathbf{R}_{ij} = \mathbf{U}_{ij} \mathbf{T}_{ij} \mathbf{V}_{ij}^\top$ , where  $\mathbf{T}_{ij}$  is rectangular diagonal with singular values  $1 > t_{ij,1} \geq \dots \geq t_{ij,r} > 0$  on its diagonal and zeros afterwards. Introduce canonical coordinates (cf. Equation 6)

$$\mathbf{u} := \mathbf{U}_{ij}^\top \mathbf{W}_i \mathbf{s}_i, \quad \mathbf{v} := \mathbf{V}_{ij}^\top \mathbf{W}_j \mathbf{s}_j.$$

Then  $\text{Cov}(\mathbf{u}) = \text{Cov}(\mathbf{v}) = \mathbf{I}$  and  $\text{Cov}(\mathbf{u}, \mathbf{v}) = \mathbf{T}_{ij}$ . Moreover, by Lemma 1, the joint density factorizes so that only the first  $r$  coordinate pairs  $(u_k, v_k)$  are correlated, while all remaining coordinates are independent standard normals.

**Step 3: Hermite diagonalization of cross-view correlations.** Let  $\{\psi_n\}_{n \geq 0}$  be the normalized univariate Hermite polynomials. For  $\mathbf{n} = (n_1, \dots, n_r) \in \mathbb{N}^r$  define

$$\Psi_{\mathbf{n}}(\mathbf{u}) := \prod_{k=1}^r \psi_{n_k}(u_k), \quad \Psi_{\mathbf{n}}(\mathbf{v}) := \prod_{k=1}^r \psi_{n_k}(v_k).$$

By Lemma 2 (Mehler–Hermite expansion) and orthonormality of Hermites, for all  $\mathbf{n}, \mathbf{m} \in \mathbb{N}^r$ ,

$$\mathbb{E}[\Psi_{\mathbf{n}}(\mathbf{u}) \Psi_{\mathbf{m}}(\mathbf{v})] = t_{\mathbf{n}} \delta_{\mathbf{n}\mathbf{m}}, \quad t_{\mathbf{n}} := \prod_{k=1}^r t_{ij,k}^{n_k}. \quad (25)$$

In particular, for the first-order multi-indices  $\mathbf{e}_k$  we have  $\Psi_{\mathbf{e}_k}(\mathbf{u}) = \psi_1(u_k) = u_k$  and  $\Psi_{\mathbf{e}_k}(\mathbf{v}) = v_k$ , with  $\mathbb{E}[u_k v_k] = t_{ij,k}$ .

**Step 4: Rewrite the CCA objective in coefficient form.** Define the whitened source-domain maximizers as functions of  $(\mathbf{u}, \mathbf{v})$ :

$$\tilde{\mathbf{f}}^*(\mathbf{u}) := \tilde{\mathbf{h}}_i^*(\mathbf{W}_i^{-1} \mathbf{U}_{ij} \mathbf{u}), \quad \tilde{\mathbf{g}}^*(\mathbf{v}) := \tilde{\mathbf{h}}_j^*(\mathbf{W}_j^{-1} \mathbf{V}_{ij} \mathbf{v}).$$

These satisfy  $\text{Cov}(\tilde{\mathbf{f}}^*(\mathbf{u})) = \text{Cov}(\tilde{\mathbf{g}}^*(\mathbf{v})) = \mathbf{I}$ . For each coordinate  $p \in [d_{\mathcal{Z}}]$ , expand the (mean-zero) component functions in the orthonormal Hermite basis on the correlated coordinates:

$$\tilde{f}_p^*(\mathbf{u}) = \sum_{\mathbf{n} \neq \mathbf{0}} \alpha_{p,\mathbf{n}} \Psi_{\mathbf{n}}(\mathbf{u}), \quad \tilde{g}_q^*(\mathbf{v}) = \sum_{\mathbf{n} \neq \mathbf{0}} \beta_{q,\mathbf{n}} \Psi_{\mathbf{n}}(\mathbf{v}).$$

Let  $\mathbf{C}_i := (\alpha_{p,\mathbf{n}})_{p,\mathbf{n}}$  and  $\mathbf{C}_j := (\beta_{q,\mathbf{n}})_{q,\mathbf{n}}$  denote the (possibly infinite) coefficient matrices whose rows collect the coefficient vectors. Whitening implies row-orthonormality (cf. the whitening-induced canonicalization Equation 4):

$$\mathbf{C}_i \mathbf{C}_i^\top = \mathbf{I}, \quad \mathbf{C}_j \mathbf{C}_j^\top = \mathbf{I}.$$

Using Equation 25, the cross-covariance of the whitened representations becomes

$$\tilde{\Sigma}_{ij}^* := \text{Cov}(\tilde{\mathbf{h}}_i^*(\mathbf{s}_i), \tilde{\mathbf{h}}_j^*(\mathbf{s}_j)) = \text{Cov}(\tilde{\mathbf{f}}^*(\mathbf{u}), \tilde{\mathbf{g}}^*(\mathbf{v})) = \mathbf{C}_i \mathbf{D} \mathbf{C}_j^\top,$$

where  $\mathbf{D} := \text{diag}((t_{\mathbf{n}})_{\mathbf{n} \neq \mathbf{0}})$  is diagonal (and trace-class since  $t_{ij,k} \in (0, 1)$  implies  $\sum_{\mathbf{n} \neq \mathbf{0}} t_{\mathbf{n}} < \infty$ ). Thus,

$$J_{ij}(\tilde{\mathbf{h}}_i^*, \tilde{\mathbf{h}}_j^*) = \|\tilde{\Sigma}_{ij}^*\|_* = \|\mathbf{C}_i \mathbf{D} \mathbf{C}_j^\top\|_*.$$

**Step 5: Optimality and recovery of the linear canonical subspaces.** We first upper bound  $\|\mathbf{C}_i \mathbf{D} \mathbf{C}_j^\top\|_*$ . Using nuclear norm duality  $\|\mathbf{M}\|_* = \sup_{\|\mathbf{Q}\|_2 \leq 1} \text{tr}(\mathbf{Q}^\top \mathbf{M})$ , together with  $\|\mathbf{C}_i\|_2 = \|\mathbf{C}_j\|_2 = 1$  (since they have orthonormal rows), we have

$$\|\mathbf{C}_i \mathbf{D} \mathbf{C}_j^\top\|_* = \sup_{\|\mathbf{Q}\|_2 \leq 1} \text{tr}((\mathbf{C}_i^\top \mathbf{Q} \mathbf{C}_j)^\top \mathbf{D}) \leq \sup_{\|\mathbf{H}\|_2 \leq 1} \text{tr}(\mathbf{H}^\top \mathbf{D}) = \|\mathbf{D}\|_* = \sum_{\mathbf{n} \neq \mathbf{0}} t_{\mathbf{n}}.$$

This upper bound is achievable in the limit  $d_{\mathcal{Z}} \rightarrow \infty$  by taking the representations to be (an enumeration of) the Hermite basis itself, i.e.,  $\tilde{\mathbf{f}}(\mathbf{u}) = (\Psi_{\mathbf{n}}(\mathbf{u}))_{\mathbf{n} \neq \mathbf{0}}$  and  $\tilde{\mathbf{g}}(\mathbf{v}) = (\Psi_{\mathbf{n}}(\mathbf{v}))_{\mathbf{n} \neq \mathbf{0}}$ , for which  $\mathbf{C}_i = \mathbf{C}_j = \mathbf{I}$  and hence  $\tilde{\Sigma}_{ij} = \mathbf{D}$ . Therefore the population optimum equals  $\|\mathbf{D}\|_*$ , and any whitened population maximizer must achieve the same value.

At this point we invoke the standard CCA canonicalization convention: because the objective and whitening constraints are invariant under within-view orthogonal post-transformations of the *feature coordinates*, we may choose an equivalent maximizer (within the unavoidable CCA orthogonal ambiguity) whose cross-covariance is diagonalized and whose coordinates form a singular basis of the diagonal operator  $\mathbf{D}$  (i.e., a basis of Hermite modes; see Equation 25). Under this canonical representative, the  $r$  first-order Hermite modes  $\{\Psi_{\mathbf{e}_k}\}_{k=1}^r$  appear among the feature coordinates, and  $\Psi_{\mathbf{e}_k}(\mathbf{u}) = u_k$ ,  $\Psi_{\mathbf{e}_k}(\mathbf{v}) = v_k$ .

Let  $\mathbf{P}_r$  be the coordinate-selection matrix that extracts exactly those  $r$  coordinates corresponding to  $\{\Psi_{\mathbf{e}_k}\}_{k=1}^r$ . Since the extracted coordinates form an orthonormal basis of the linear subspace  $\text{span}\{u_1, \dots, u_r\}$  (resp.  $\text{span}\{v_1, \dots, v_r\}$ ), there exist  $\mathbf{O}_i, \mathbf{O}_j \in O(r)$  such that

$$\mathbf{P}_r \tilde{\mathbf{f}}^*(\mathbf{u}) = \mathbf{O}_i \mathbf{u}[1:r], \quad \mathbf{P}_r \tilde{\mathbf{g}}^*(\mathbf{v}) = \mathbf{O}_j \mathbf{v}[1:r].$$

Finally, substituting back  $\mathbf{u} = \mathbf{U}_{ij}^\top \mathbf{W}_i \mathbf{s}_i$  and  $\mathbf{v} = \mathbf{V}_{ij}^\top \mathbf{W}_j \mathbf{s}_j$  yields

$$\mathbf{P}_r \tilde{\mathbf{h}}_i^*(\mathbf{s}_i) = \mathbf{O}_i \mathbf{U}_{ij}(:, 1:r)^\top \mathbf{W}_i \mathbf{s}_i, \quad \mathbf{P}_r \tilde{\mathbf{h}}_j^*(\mathbf{s}_j) = \mathbf{O}_j \mathbf{V}_{ij}(:, 1:r)^\top \mathbf{W}_j \mathbf{s}_j,$$

which is exactly Equation 7.

**Consequence (subspace identification).** The right-hand sides lie in  $\text{col}(\mathbf{U}_{ij}(:, 1:r)) = \mathcal{U}_{i|j}$  and  $\text{col}(\mathbf{V}_{ij}(:, 1:r)) = \mathcal{U}_{j|i}$ , respectively, and the only remaining ambiguity is the orthogonal mixing  $\mathbf{O}_i, \mathbf{O}_j$  inside these  $r$ -dimensional subspaces. Hence the maximizers identify the whitened correlated subspaces up to orthogonal transformations.  $\square$

## 11 Proof of Corollary 1

*Proof of Corollary 1.* Fix a pair of views  $i \neq j$  and write  $r := r_{ij}$  and  $d := d_{\mathcal{Z}}$ , with  $d \geq r$ . By reparameterization invariance (Lemma 6), it suffices to analyze the *source-domain* problem: maximize the two-view CCA objective over whitened mappings  $\tilde{\mathbf{h}}_i, \tilde{\mathbf{h}}_j$  with  $\mathbb{E}[\tilde{\mathbf{h}}_\ell] = \mathbf{0}$  and  $\text{Cov}(\tilde{\mathbf{h}}_\ell) = \mathbf{I}_d$  for  $\ell \in \{i, j\}$ .

Let  $(\mathbf{u}, \mathbf{v})$  be the canonical coordinates from Lemma 1,

$$\mathbf{u} = \mathbf{U}_{ij}^\top \mathbf{W}_i \mathbf{s}_i, \quad \mathbf{v} = \mathbf{V}_{ij}^\top \mathbf{W}_j \mathbf{s}_j,$$

and denote  $\mathbf{u}_{1:r} := (u_1, \dots, u_r)^\top$  and  $\mathbf{v}_{1:r} := (v_1, \dots, v_r)^\top$ . Let  $\{\Psi_{\mathbf{n}}\}_{\mathbf{n} \in \mathbb{N}^r}$  be the normalized multivariate Hermite basis from Lemma 2, and define  $t_{\mathbf{n}} := \prod_{k=1}^r t_{ij,k}^{n_k}$ . (We always exclude  $\mathbf{n} = \mathbf{0}$  below, because mean-zero constraints remove the constant mode.)

**Step 1: Diagonal cross-moments in the Hermite basis.** From Lemma 2 and the orthonormality of  $\{\Psi_{\mathbf{n}}\}$  in  $L^2(\phi)$ , we obtain for any  $\mathbf{n}, \mathbf{m} \in \mathbb{N}^r$ ,

$$\begin{aligned} \mathbb{E}[\Psi_{\mathbf{n}}(\mathbf{u}_{1:r}) \Psi_{\mathbf{m}}(\mathbf{v}_{1:r})] &= \int \Psi_{\mathbf{n}}(\mathbf{u}) \Psi_{\mathbf{m}}(\mathbf{v}) \phi(\mathbf{u}) \phi(\mathbf{v}) \sum_{\ell \in \mathbb{N}^r} t_{\ell} \Psi_{\ell}(\mathbf{u}) \Psi_{\ell}(\mathbf{v}) d\mathbf{u} d\mathbf{v} \\ &= \sum_{\ell \in \mathbb{N}^r} t_{\ell} \left( \int \Psi_{\mathbf{n}}(\mathbf{u}) \Psi_{\ell}(\mathbf{u}) \phi(\mathbf{u}) d\mathbf{u} \right) \left( \int \Psi_{\mathbf{m}}(\mathbf{v}) \Psi_{\ell}(\mathbf{v}) \phi(\mathbf{v}) d\mathbf{v} \right) \\ &= t_{\mathbf{n}} \delta_{\mathbf{nm}}. \end{aligned} \tag{26}$$

**Step 2: Coefficient representation of feasible whitened maps.** Let  $(\tilde{\mathbf{h}}_i, \tilde{\mathbf{h}}_j)$  be any feasible whitened pair in  $L^2$  with output dimension  $d$ . Expand each coordinate in the orthonormal basis: for  $p, q \in [d]$ ,

$$\tilde{h}_{i,p}(\mathbf{u}_{1:r}) = \sum_{\mathbf{n} \neq \mathbf{0}} a_{p,\mathbf{n}} \Psi_{\mathbf{n}}(\mathbf{u}_{1:r}), \quad \tilde{h}_{j,q}(\mathbf{v}_{1:r}) = \sum_{\mathbf{n} \neq \mathbf{0}} b_{q,\mathbf{n}} \Psi_{\mathbf{n}}(\mathbf{v}_{1:r}),$$

where  $\mathbf{n} = \mathbf{0}$  is absent because  $\mathbb{E}[\tilde{h}_{i,p}] = \mathbb{E}[\tilde{h}_{j,q}] = 0$ . Let  $\mathbf{A} = [a_{p,\mathbf{n}}]_{p,\mathbf{n}}$  and  $\mathbf{B} = [b_{q,\mathbf{n}}]_{q,\mathbf{n}}$ . By whitening-induced canonicalization (Equation 4), the coefficient rows are orthonormal:

$$\mathbf{A}\mathbf{A}^\top = \mathbf{I}_d, \quad \mathbf{B}\mathbf{B}^\top = \mathbf{I}_d. \quad (27)$$

Using Equation 26, the cross-covariance matrix  $\mathbf{C} := \text{Cov}(\tilde{\mathbf{h}}_i(\mathbf{u}_{1:r}), \tilde{\mathbf{h}}_j(\mathbf{v}_{1:r}))$  satisfies

$$C_{pq} = \mathbb{E}[\tilde{h}_{i,p}(\mathbf{u}_{1:r}) \tilde{h}_{j,q}(\mathbf{v}_{1:r})] = \sum_{\mathbf{n} \neq \mathbf{0}} a_{p,\mathbf{n}} b_{q,\mathbf{n}} t_{\mathbf{n}}, \quad \iff \quad \mathbf{C} = \mathbf{A}\mathbf{T}\mathbf{B}^\top, \quad (28)$$

where  $\mathbf{T}$  is diagonal with diagonal entries  $\{t_{\mathbf{n}}\}_{\mathbf{n} \neq \mathbf{0}}$ .

**Step 3: A Ky Fan (nuclear-norm) upper bound.** Let  $t_{(1)} \geq t_{(2)} \geq \dots$  be the nonincreasing rearrangement of  $\{t_{\mathbf{n}}\}_{\mathbf{n} \neq \mathbf{0}}$ . Then for any  $\mathbf{A}, \mathbf{B}$  satisfying Equation 27,

$$\|\mathbf{C}\|_* = \|\mathbf{A}\mathbf{T}\mathbf{B}^\top\|_* \leq \sum_{k=1}^d t_{(k)}. \quad (29)$$

Indeed, by the Ky Fan variational characterization of the nuclear norm,

$$\|\mathbf{A}\mathbf{T}\mathbf{B}^\top\|_* = \max_{\mathbf{U}, \mathbf{V} \in O(d)} \text{Tr}(\mathbf{U}^\top \mathbf{A}\mathbf{T}\mathbf{B}^\top \mathbf{V}) = \max_{\mathbf{U}, \mathbf{V} \in O(d)} \text{Tr}((\mathbf{A}^\top \mathbf{U})^\top \mathbf{T}(\mathbf{B}^\top \mathbf{V})).$$

By Equation 27, both  $\mathbf{A}^\top \mathbf{U}$  and  $\mathbf{B}^\top \mathbf{V}$  have orthonormal columns, so the last quantity is bounded by the Ky Fan  $d$ -norm of  $\mathbf{T}$ , i.e.  $\sum_{k=1}^d \sigma_k(\mathbf{T}) = \sum_{k=1}^d t_{(k)}$ , proving Equation 29. Moreover, the bound is achievable by choosing  $\mathbf{A}, \mathbf{B}$  to select the  $d$  Hermite modes with largest  $t_{\mathbf{n}}$ .

**Step 4: First-order dominance separates linear from higher-order modes.** For any multi-index  $\mathbf{n} \neq \mathbf{0}$  with total degree  $|\mathbf{n}| := \sum_{k=1}^r n_k \geq 2$ ,

$$t_{\mathbf{n}} = \prod_{k=1}^r t_{ij,k}^{n_k} \leq t_{ij,1}^{|\mathbf{n}|} \leq t_{ij,1}^2,$$

since  $0 \leq t_{ij,k} \leq t_{ij,1} < 1$ . On the other hand, for the  $r$  first-order indices  $\mathbf{e}_k$  we have  $t_{\mathbf{e}_k} = t_{ij,k}$ . If  $r \geq 2$ , Assumption 2 gives  $t_{ij,r} > t_{ij,1}^2$ ; if  $r = 1$ , the strict inequality  $t_{ij,1} > t_{ij,1}^2$  holds automatically because  $t_{ij,1} \in (0, 1)$ . Therefore,

$$t_{ij,r} > t_{ij,1}^2 \geq t_{\mathbf{n}} \quad \forall \mathbf{n} \neq \mathbf{0} \text{ with } |\mathbf{n}| \geq 2.$$

Consequently, the  $r$  largest values among  $\{t_{\mathbf{n}}\}_{\mathbf{n} \neq \mathbf{0}}$  are exactly  $\{t_{ij,1}, \dots, t_{ij,r}\}$ , attained by the first-order Hermite modes  $\{\Psi_{\mathbf{e}_1}, \dots, \Psi_{\mathbf{e}_r}\}$  (which are linear functions of  $\mathbf{u}_{1:r}$ ).

**Step 5: Conclusion and explicit selector.** Let  $(\tilde{\mathbf{h}}_i^*, \tilde{\mathbf{h}}_j^*)$  be any population maximizer with finite  $d \geq r$  and let  $\mathbf{C}^* = \text{Cov}(\tilde{\mathbf{h}}_i^*, \tilde{\mathbf{h}}_j^*)$ . By Equation 29 and attainability, the optimal value equals  $\sum_{k=1}^d t_{(k)}$ . By Step 4, the top  $r$  singular values of the optimal correlation structure must therefore come from the first-order modes, and these modes are strictly separated from all higher-order ones by the gap  $t_{ij,r} - t_{ij,1}^2 > 0$ .

Now use the post-orthogonal closure of the whitened class (Definition 2): take an SVD  $\mathbf{C}^* = \mathbf{Q}_i \text{diag}(\sigma_1, \dots, \sigma_d) \mathbf{Q}_j^\top$  and replace  $\tilde{\mathbf{h}}_i^*, \tilde{\mathbf{h}}_j^*$  by  $\mathbf{Q}_i^\top \tilde{\mathbf{h}}_i^*$  and  $\mathbf{Q}_j^\top \tilde{\mathbf{h}}_j^*$ . This produces another maximizer (same objective value) whose cross-covariance is diagonal with  $\sigma_1 \geq \dots \geq \sigma_d$ . By Step 4 and  $d \geq r$ , the first  $r$  diagonal entries correspond to the first-order Hermite subspaces, hence there exist  $\mathbf{O}_i, \mathbf{O}_j \in O(r)$  such that,  $P$ -a.s.,

$$\mathbf{P}_r \tilde{\mathbf{h}}_i^*(\mathbf{s}_i) = \mathbf{O}_i \mathbf{u}_{1:r}, \quad \mathbf{P}_r \tilde{\mathbf{h}}_j^*(\mathbf{s}_j) = \mathbf{O}_j \mathbf{v}_{1:r},$$

with the explicit selector

$$\mathbf{P}_r := [\mathbf{I}_r \ \mathbf{0}] \in \mathbb{R}^{r \times d}.$$

Finally, substituting  $\mathbf{u}_{1:r} = \mathbf{U}_{ij}(:, 1:r)^\top \mathbf{W}_i \mathbf{s}_i$  and  $\mathbf{v}_{1:r} = \mathbf{V}_{ij}(:, 1:r)^\top \mathbf{W}_j \mathbf{s}_j$  yields exactly Equation 7 with  $\mathbf{P}_{r_{ij}} = \mathbf{P}_r$ .  $\square$

---

## 12 Proof of Theorem 5.2

*Proof of Theorem 5.2.* We work entirely in the source domain using the induced whitened mappings

$$\tilde{\mathbf{h}}_i := \tilde{\mathbf{f}}_i \circ \mathbf{g}_i, \quad i \in [N].$$

By reparameterization invariance (Lemma 6), optimizing Equation 2 over  $\{\tilde{\mathbf{f}}_i\}$  is equivalent to optimizing it over  $\{\tilde{\mathbf{h}}_i\}$ , and each  $\tilde{\mathbf{h}}_i$  satisfies

$$\mathbb{E}[\tilde{\mathbf{h}}_i(\mathbf{s}_i)] = \mathbf{0}, \quad \text{Cov}(\tilde{\mathbf{h}}_i(\mathbf{s}_i)) = \mathbf{I}.$$

Define the pairwise objectives

$$J_{ij}(\tilde{\mathbf{h}}_i, \tilde{\mathbf{h}}_j) := \left\| \text{Cov}(\tilde{\mathbf{h}}_i(\mathbf{s}_i), \tilde{\mathbf{h}}_j(\mathbf{s}_j)) \right\|_*, \quad 1 \leq i < j \leq N,$$

so that

$$J(\tilde{\mathbf{h}}_1, \dots, \tilde{\mathbf{h}}_N) = \sum_{1 \leq i < j \leq N} J_{ij}(\tilde{\mathbf{h}}_i, \tilde{\mathbf{h}}_j).$$

### Step 1: Pairwise optimality of a multi-view maximizer.

Let

$$M_{ij} := \sup_{\tilde{\mathbf{h}}_i, \tilde{\mathbf{h}}_j \text{ whitened}} J_{ij}(\tilde{\mathbf{h}}_i, \tilde{\mathbf{h}}_j)$$

be the two-view population optimum (with  $d_{\mathcal{Z}} \rightarrow \infty$ ). For any feasible collection,

$$J(\tilde{\mathbf{h}}_1, \dots, \tilde{\mathbf{h}}_N) \leq \sum_{i < j} M_{ij}.$$

Under item 1.2, by the canonical factorization (Lemma 1) and the Mehler–Hermite expansion (Lemma 2), the cross-covariance operator between two views admits a diagonal spectral decomposition in the multivariate Hermite basis, with singular values  $\{t_{\mathbf{n}}\}$ . The corresponding singular functions achieve

$$J_{ij} = \sum_{\mathbf{n}} t_{\mathbf{n}} = M_{ij}.$$

Thus the upper bound  $\sum_{i < j} M_{ij}$  is attainable.

Therefore, if  $\{\tilde{\mathbf{h}}_i^*\}_{i=1}^N$  is a global maximizer of  $J$ , we must have

$$J_{ij}(\tilde{\mathbf{h}}_i^*, \tilde{\mathbf{h}}_j^*) = M_{ij}, \quad \forall 1 \leq i < j \leq N. \quad (30)$$

Hence every pair  $(\tilde{\mathbf{h}}_i^*, \tilde{\mathbf{h}}_j^*)$  is a two-view population maximizer.

### Step 2: Apply two-view subspace identifiability.

Fix  $i \neq j$  and let  $r_{ij} = \text{rank}(\mathbf{A}_i \mathbf{A}_j^\top)$ . By Theorem 5.1, there exists  $\mathbf{O}_{i|j} \in O(r_{ij})$  and a selection matrix  $\mathbf{P}_{r_{ij}}^{(i|j)}$  such that

$$\mathbf{P}_{r_{ij}}^{(i|j)} \tilde{\mathbf{h}}_i^*(\mathbf{s}_i) = \mathbf{O}_{i|j} \mathbf{U}_{ij}(:, 1 : r_{ij})^\top \mathbf{W}_i \mathbf{s}_i. \quad (31)$$

Thus, for each fixed  $i$  and every  $j \neq i$ , the representation contains an  $r_{ij}$ -dimensional block identifying the pairwise correlated subspace  $\mathcal{U}_{i|j}$ .

### Step 3: Extract the multi-view intersection.

By Definition 1,

$$\mathcal{U}_i^{\text{mv}} = \bigcap_{j \neq i} \mathcal{U}_{i|j}, \quad r_i = \dim(\mathcal{U}_i^{\text{mv}}).$$

Let  $\mathbf{U}_i^{\text{mv}} \in \mathbb{R}^{d_{\mathcal{S}_i} \times r_i}$  be an orthonormal basis of  $\mathcal{U}_i^{\text{mv}}$ .

Since  $\mathcal{U}_i^{\text{mv}} \subseteq \mathcal{U}_{i|j_0}$  for any fixed  $j_0 \neq i$ , there exists  $\mathbf{B}_i \in \mathbb{R}^{r_{ij_0} \times r_i}$  with orthonormal columns such that

$$\mathbf{U}_i^{\text{mv}} = \mathbf{U}_{ij_0}(:, 1 : r_{ij_0})\mathbf{B}_i.$$

Multiplying Equation 31 (on pair  $(i, j_0)$ ) by  $\mathbf{B}_i^\top \mathbf{O}_{i|j_0}^\top$  gives

$$\mathbf{B}_i^\top \mathbf{O}_{i|j_0}^\top \mathbf{P}_{r_{ij_0}}^{(i|j_0)} \tilde{\mathbf{h}}_i^*(\mathbf{s}_i) = (\mathbf{U}_i^{\text{mv}})^\top \mathbf{W}_i \mathbf{s}_i.$$

Define

$$\mathbf{P}_{r_i} := \mathbf{B}_i^\top \mathbf{O}_{i|j_0}^\top \mathbf{P}_{r_{ij_0}}^{(i|j_0)} \in \mathbb{R}^{r_i \times d_{\mathcal{Z}}}.$$

Then

$$\mathbf{P}_{r_i} \tilde{\mathbf{h}}_i^*(\mathbf{s}_i) = (\mathbf{U}_i^{\text{mv}})^\top \mathbf{W}_i \mathbf{s}_i. \quad (32)$$

Since  $\mathbf{U}_i^{\text{mv}}$  is defined only up to an orthogonal change of basis, absorbing that change into  $\mathbf{O}_i \in O(r_i)$  yields

$$\mathbf{P}_{r_i} \tilde{\mathbf{h}}_i^*(\mathbf{s}_i) = \mathbf{O}_i (\mathbf{U}_i^{\text{mv}})^\top \mathbf{W}_i \mathbf{s}_i.$$

### Conclusion.

Equation 8 holds for every  $i \in [N]$ . Hence the multi-view population maximizers identify the jointly correlated subspaces  $\mathcal{U}_i^{\text{mv}}$  up to view-specific orthogonal transformations.  $\square$

## 13 Proof of Corollary 2

*Proof of Corollary 2.* Fix an arbitrary  $i \in [N]$ . Recall that  $\mathbf{P}_{i|j}$  and  $\hat{\mathbf{P}}_{i|j}$  denote the orthogonal projectors onto  $\mathcal{U}_{i|j}$  and  $\hat{\mathcal{U}}_{i|j}$ , respectively, and

$$\mathbf{S}_i := \frac{1}{N-1} \sum_{j \neq i} \mathbf{P}_{i|j}, \quad \hat{\mathbf{S}}_i := \frac{1}{N-1} \sum_{j \neq i} \hat{\mathbf{P}}_{i|j}.$$

**Step 1: Spectral characterization of  $\mathcal{U}_i^{\text{mv}}$ .** We first show that  $\mathcal{U}_i^{\text{mv}} = \bigcap_{j \neq i} \mathcal{U}_{i|j}$  coincides with the eigenspace of  $\mathbf{S}_i$  associated with eigenvalue 1.

( $\subseteq$ ) If  $\mathbf{v} \in \mathcal{U}_i^{\text{mv}}$ , then  $\mathbf{P}_{i|j} \mathbf{v} = \mathbf{v}$  for all  $j \neq i$ , hence

$$\mathbf{S}_i \mathbf{v} = \frac{1}{N-1} \sum_{j \neq i} \mathbf{P}_{i|j} \mathbf{v} = \frac{1}{N-1} \sum_{j \neq i} \mathbf{v} = \mathbf{v},$$

so  $\mathbf{v}$  lies in the 1-eigenspace of  $\mathbf{S}_i$ .

( $\supseteq$ ) Conversely, suppose  $\mathbf{S}_i \mathbf{v} = \mathbf{v}$ . Taking inner products,

$$\|\mathbf{v}\|_2^2 = \mathbf{v}^\top \mathbf{S}_i \mathbf{v} = \frac{1}{N-1} \sum_{j \neq i} \mathbf{v}^\top \mathbf{P}_{i|j} \mathbf{v} = \frac{1}{N-1} \sum_{j \neq i} \|\mathbf{P}_{i|j} \mathbf{v}\|_2^2. \quad (33)$$

Since  $\mathbf{P}_{i|j}$  is an orthogonal projector,  $\|\mathbf{P}_{i|j} \mathbf{v}\|_2 \leq \|\mathbf{v}\|_2$  for every  $j$ . Thus the average in Equation 33 can equal  $\|\mathbf{v}\|_2^2$  only if  $\|\mathbf{P}_{i|j} \mathbf{v}\|_2 = \|\mathbf{v}\|_2$  for all  $j \neq i$ , which forces  $\mathbf{P}_{i|j} \mathbf{v} = \mathbf{v}$  for all  $j \neq i$ . Hence  $\mathbf{v} \in \bigcap_{j \neq i} \mathcal{U}_{i|j} = \mathcal{U}_i^{\text{mv}}$ .

Therefore, the 1-eigenspace of  $\mathbf{S}_i$  is exactly  $\mathcal{U}_i^{\text{mv}}$ . In particular, if  $r_i = \dim(\mathcal{U}_i^{\text{mv}})$ , then  $\lambda_1(\mathbf{S}_i) = \dots = \lambda_{r_i}(\mathbf{S}_i) = 1$  and

$$\Gamma_i := 1 - \lambda_{r_i+1}(\mathbf{S}_i) = \lambda_{r_i}(\mathbf{S}_i) - \lambda_{r_i+1}(\mathbf{S}_i) > 0.$$

**Step 2: Davis–Kahan for the first inequality.** Both  $\mathbf{S}_i$  and  $\hat{\mathbf{S}}_i$  are symmetric. Let  $\mathcal{U}_i^{\text{mv}}$  be the invariant subspace of  $\mathbf{S}_i$  corresponding to the eigenvalue cluster at 1 (multiplicity  $r_i$ ), and let  $\hat{\mathcal{U}}_i^{\text{mv}}$  be the top- $r_i$  eigenspace of  $\hat{\mathbf{S}}_i$ . By the Davis–Kahan sin  $\Theta$  theorem for symmetric matrices applied to the eigen-gap  $\Gamma_i = \lambda_{r_i}(\mathbf{S}_i) - \lambda_{r_i+1}(\mathbf{S}_i)$ ,

$$\|\sin \Theta(\hat{\mathcal{U}}_i^{\text{mv}}, \mathcal{U}_i^{\text{mv}})\|_2 \leq \frac{\|\hat{\mathbf{S}}_i - \mathbf{S}_i\|_2}{\Gamma_i},$$

which is the first displayed inequality.

**Step 3: Bounding  $\|\widehat{\mathbf{S}}_i - \mathbf{S}_i\|_2$  by pairwise errors.** By linearity and the triangle inequality,

$$\|\widehat{\mathbf{S}}_i - \mathbf{S}_i\|_2 = \left\| \frac{1}{N-1} \sum_{j \neq i} (\widehat{\mathbf{P}}_{i|j} - \mathbf{P}_{i|j}) \right\|_2 \leq \frac{1}{N-1} \sum_{j \neq i} \|\widehat{\mathbf{P}}_{i|j} - \mathbf{P}_{i|j}\|_2 \leq \max_{j \neq i} \|\widehat{\mathbf{P}}_{i|j} - \mathbf{P}_{i|j}\|_2.$$

It remains to relate projector error to principal-angle error. Fix  $j \neq i$  and let  $\mathbf{U}, \widehat{\mathbf{U}}$  be orthonormal basis matrices for  $\mathcal{U}_{i|j}$  and  $\widehat{\mathcal{U}}_{i|j}$ , respectively, so that  $\mathbf{P} := \mathbf{U}\mathbf{U}^\top$  and  $\widehat{\mathbf{P}} := \widehat{\mathbf{U}}\widehat{\mathbf{U}}^\top$ . Use the identity

$$\widehat{\mathbf{P}} - \mathbf{P} = (\mathbf{I} - \mathbf{P})\widehat{\mathbf{P}} - \mathbf{P}(\mathbf{I} - \widehat{\mathbf{P}}),$$

hence

$$\|\widehat{\mathbf{P}} - \mathbf{P}\|_2 \leq \|(\mathbf{I} - \mathbf{P})\widehat{\mathbf{P}}\|_2 + \|\mathbf{P}(\mathbf{I} - \widehat{\mathbf{P}})\|_2.$$

Since  $\widehat{\mathbf{P}}$  is a projector onto  $\text{col}(\widehat{\mathbf{U}})$ ,

$$\|(\mathbf{I} - \mathbf{P})\widehat{\mathbf{P}}\|_2 = \|(\mathbf{I} - \mathbf{P})\widehat{\mathbf{U}}\|_2 = \|\sin \Theta(\widehat{\mathcal{U}}_{i|j}, \mathcal{U}_{i|j})\|_2,$$

and similarly

$$\|\mathbf{P}(\mathbf{I} - \widehat{\mathbf{P}})\|_2 = \|(\mathbf{I} - \widehat{\mathbf{P}})\mathbf{U}\|_2 = \|\sin \Theta(\widehat{\mathcal{U}}_{i|j}, \mathcal{U}_{i|j})\|_2.$$

Therefore,

$$\|\widehat{\mathbf{P}}_{i|j} - \mathbf{P}_{i|j}\|_2 \leq 2 \|\sin \Theta(\widehat{\mathcal{U}}_{i|j}, \mathcal{U}_{i|j})\|_2.$$

Taking the maximum over  $j \neq i$  and combining with the previous display yields

$$\|\widehat{\mathbf{S}}_i - \mathbf{S}_i\|_2 \leq 2 \max_{j \neq i} \|\sin \Theta(\widehat{\mathcal{U}}_{i|j}, \mathcal{U}_{i|j})\|_2.$$

Plugging this into Step 2 proves the second displayed inequality:

$$\|\sin \Theta(\widehat{\mathcal{U}}_i^{\text{mv}}, \mathcal{U}_i^{\text{mv}})\|_2 \leq \frac{\|\widehat{\mathbf{S}}_i - \mathbf{S}_i\|_2}{\Gamma_i} \leq \frac{2}{\Gamma_i} \max_{j \neq i} \|\sin \Theta(\widehat{\mathcal{U}}_{i|j}, \mathcal{U}_{i|j})\|_2.$$

**Step 4:  $O_{\mathbb{P}}(n^{-1/2})$  consistency.** By Theorem 5.3,  $\|\widehat{\mathbf{R}}_{ij} - \mathbf{R}_{ij}\|_2 = O_{\mathbb{P}}(n^{-1/2})$  uniformly over pairs, and on the event  $\|\widehat{\mathbf{R}}_{ij} - \mathbf{R}_{ij}\|_2 \leq \Delta_{ij}/2$ ,

$$\|\sin \Theta(\widehat{\mathcal{U}}_{i|j}, \mathcal{U}_{i|j})\|_2 \leq \frac{2\|\widehat{\mathbf{R}}_{ij} - \mathbf{R}_{ij}\|_2}{\Delta_{ij}} = O_{\mathbb{P}}(n^{-1/2}),$$

with constants governed by  $\Delta_{ij}$ . Substituting into the inequality proved above shows that

$$\|\sin \Theta(\widehat{\mathcal{U}}_i^{\text{mv}}, \mathcal{U}_i^{\text{mv}})\|_2 = O_{\mathbb{P}}(n^{-1/2}),$$

with the pre-constant depending on  $\Gamma_i^{-1}$  and  $\{\Delta_{ij}^{-1}\}_{j \neq i}$ , as claimed.  $\square$

## 14 Proof of Theorem 5.3

*Proof of Theorem 5.3.* Fix  $d := d_{\mathcal{Z}}$  and  $\delta \in (0, 1)$ . Recall the *population-whitened* representations

$$\tilde{\mathbf{z}}_i := \boldsymbol{\Sigma}_{ii}^{-1/2}(\mathbf{z}_i - \mathbb{E}[\mathbf{z}_i]), \quad \text{Cov}(\tilde{\mathbf{z}}_i) = \mathbf{I}_d,$$

and note that the population normalized cross-covariance is precisely

$$\mathbf{R}_{ij} = \boldsymbol{\Sigma}_{ii}^{-1/2} \boldsymbol{\Sigma}_{ij} \boldsymbol{\Sigma}_{jj}^{-1/2} = \text{Cov}(\tilde{\mathbf{z}}_i, \tilde{\mathbf{z}}_j).$$

Throughout the proof, we work in these population-whitened coordinates (i.e., we replace  $\tilde{\mathbf{z}}_i$  by  $\mathbf{z}_i$  for notational simplicity). Thus we may assume

$$\mathbb{E}[\mathbf{z}_i] = \mathbf{0}, \quad \text{Cov}(\mathbf{z}_i) = \mathbf{I}_d, \quad \mathbf{R}_{ij} = \text{Cov}(\mathbf{z}_i, \mathbf{z}_j). \quad (34)$$

The empirical (cross-)covariances are defined as in the main text,

$$\widehat{\boldsymbol{\Sigma}}_{ij} := \frac{1}{n} \sum_{t=1}^n (\mathbf{z}_i^{(t)} - \bar{\mathbf{z}}_i)(\mathbf{z}_j^{(t)} - \bar{\mathbf{z}}_j)^\top, \quad \widehat{\mathbf{R}}_{ij} := \widehat{\boldsymbol{\Sigma}}_{ii}^{-1/2} \widehat{\boldsymbol{\Sigma}}_{ij} \widehat{\boldsymbol{\Sigma}}_{jj}^{-1/2}.$$

**Step 1: sub-Gaussian concentration for pairwise (cross-)covariances.** Fix a pair  $1 \leq i < j \leq N$  and define the stacked vector

$$\mathbf{y}^{(t)} := \begin{bmatrix} \mathbf{z}_i^{(t)} \\ \mathbf{z}_j^{(t)} \end{bmatrix} \in \mathbb{R}^{2d}.$$

Let  $\mathbf{v} = [\mathbf{v}_1^\top, \mathbf{v}_2^\top]^\top \in \mathbb{S}^{2d-1}$ . By the triangle inequality for the Orlicz  $\psi_2$  norm and Assumption 3,

$$\|\mathbf{v}^\top \mathbf{y}^{(t)}\|_{\psi_2} = \|\mathbf{v}_1^\top \mathbf{z}_i^{(t)} + \mathbf{v}_2^\top \mathbf{z}_j^{(t)}\|_{\psi_2} \leq \|\mathbf{v}_1^\top \mathbf{z}_i^{(t)}\|_{\psi_2} + \|\mathbf{v}_2^\top \mathbf{z}_j^{(t)}\|_{\psi_2} \leq \kappa(\|\mathbf{v}_1\|_2 + \|\mathbf{v}_2\|_2) \leq \sqrt{2}\kappa.$$

Hence  $\mathbf{y}^{(t)}$  is sub-Gaussian in  $\mathbb{R}^{2d}$  with parameter  $\lesssim \kappa$ . Its population covariance is the block matrix

$$\boldsymbol{\Sigma}_{\mathbf{y}} := \text{Cov}(\mathbf{y}^{(1)}) = \begin{pmatrix} \mathbf{I}_d & \mathbf{R}_{ij} \\ \mathbf{R}_{ij}^\top & \mathbf{I}_d \end{pmatrix}.$$

Moreover,  $\|\mathbf{R}_{ij}\|_2 \leq 1$  by Cauchy–Schwarz: for any unit  $\mathbf{a}, \mathbf{b}$ ,

$$|\mathbf{a}^\top \mathbf{R}_{ij} \mathbf{b}| = |\mathbb{E}[(\mathbf{a}^\top \mathbf{z}_i)(\mathbf{b}^\top \mathbf{z}_j)]| \leq \sqrt{\mathbb{E}(\mathbf{a}^\top \mathbf{z}_i)^2} \sqrt{\mathbb{E}(\mathbf{b}^\top \mathbf{z}_j)^2} = 1,$$

so  $\|\boldsymbol{\Sigma}_{\mathbf{y}}\|_2 \leq 2$ .

Define the *uncentered* empirical covariance  $\tilde{\boldsymbol{\Sigma}}_{\mathbf{y}} := \frac{1}{n} \sum_{t=1}^n \mathbf{y}^{(t)} \mathbf{y}^{(t)\top}$  and the centered one  $\hat{\boldsymbol{\Sigma}}_{\mathbf{y}} := \frac{1}{n} \sum_{t=1}^n (\mathbf{y}^{(t)} - \bar{\mathbf{y}})(\mathbf{y}^{(t)} - \bar{\mathbf{y}})^\top = \tilde{\boldsymbol{\Sigma}}_{\mathbf{y}} - \bar{\mathbf{y}} \bar{\mathbf{y}}^\top$ . Applying ?? to  $\{\mathbf{y}^{(t)}\}_{t=1}^n$  (with  $m = 2d$  and  $K \asymp \kappa$ ) yields that, with probability at least  $1 - \delta_{ij}/2$ ,

$$\|\tilde{\boldsymbol{\Sigma}}_{\mathbf{y}} - \boldsymbol{\Sigma}_{\mathbf{y}}\|_2 \leq c_1 \kappa^2 \left( \sqrt{\frac{2d + \log(4/\delta_{ij})}{n}} + \frac{2d + \log(4/\delta_{ij})}{n} \right), \quad (35)$$

for a universal constant  $c_1 > 0$ .

We also need to control the mean correction term  $\bar{\mathbf{y}} \bar{\mathbf{y}}^\top$ . By standard sub-Gaussian mean concentration (e.g., Vershynin, 2018), with probability at least  $1 - \delta_{ij}/2$ ,

$$\|\bar{\mathbf{y}}\|_2 \leq c_2 \kappa \sqrt{\frac{2d + \log(2/\delta_{ij})}{n}}, \quad (36)$$

for a universal  $c_2 > 0$ , hence  $\|\bar{\mathbf{y}} \bar{\mathbf{y}}^\top\|_2 = \|\bar{\mathbf{y}}\|_2^2 \leq c_2^2 \kappa^2 \frac{2d + \log(2/\delta_{ij})}{n}$ . Combining Equation 35–Equation 36 and absorbing the quadratic term into the square-root term (and using a larger universal constant when the square-root term exceeds 1), we obtain that with probability at least  $1 - \delta_{ij}$ ,

$$\|\hat{\boldsymbol{\Sigma}}_{\mathbf{y}} - \boldsymbol{\Sigma}_{\mathbf{y}}\|_2 \leq c_3 \kappa^2 \sqrt{\frac{2d + \log(4/\delta_{ij})}{n}}, \quad (37)$$

for a universal  $c_3 > 0$ .

Since each block of  $\hat{\boldsymbol{\Sigma}}_{\mathbf{y}} - \boldsymbol{\Sigma}_{\mathbf{y}}$  is a submatrix of the full difference, we have (on the same event)

$$\|\hat{\boldsymbol{\Sigma}}_{ii} - \mathbf{I}\|_2 \leq \varepsilon_{ij}, \quad \|\hat{\boldsymbol{\Sigma}}_{jj} - \mathbf{I}\|_2 \leq \varepsilon_{ij}, \quad \|\hat{\boldsymbol{\Sigma}}_{ij} - \mathbf{R}_{ij}\|_2 \leq \varepsilon_{ij}, \quad (38)$$

where

$$\varepsilon_{ij} := c_3 \kappa^2 \sqrt{\frac{2d + \log(4/\delta_{ij})}{n}}.$$

**Step 2: control of empirical whitening matrices.** Assume  $\varepsilon_{ij} < 1$ . Then Weyl’s inequality gives  $\lambda_{\min}(\hat{\boldsymbol{\Sigma}}_{ii}) \geq 1 - \varepsilon_{ij} > 0$  and similarly for  $j$ , so  $\hat{\boldsymbol{\Sigma}}_{ii}^{-1/2}$  and  $\hat{\boldsymbol{\Sigma}}_{jj}^{-1/2}$  exist. Moreover, all eigenvalues of  $\hat{\boldsymbol{\Sigma}}_{ii}$  lie in  $[1 - \varepsilon_{ij}, 1 + \varepsilon_{ij}]$ , hence those of  $\hat{\boldsymbol{\Sigma}}_{ii}^{-1/2}$  lie in  $[(1 + \varepsilon_{ij})^{-1/2}, (1 - \varepsilon_{ij})^{-1/2}]$ , and therefore

$$\|\hat{\boldsymbol{\Sigma}}_{ii}^{-1/2}\|_2 \leq (1 - \varepsilon_{ij})^{-1/2}, \quad \|\hat{\boldsymbol{\Sigma}}_{ii}^{-1/2} - \mathbf{I}\|_2 \leq (1 - \varepsilon_{ij})^{-1/2} - 1 \leq \frac{\varepsilon_{ij}}{1 - \varepsilon_{ij}}. \quad (39)$$

The same bounds hold for  $\hat{\boldsymbol{\Sigma}}_{jj}^{-1/2}$ .

**Step 3: concentration of  $\widehat{\mathbf{R}}_{ij}$ .** Write  $\mathbf{A}_i := \widehat{\Sigma}_{ii}^{-1/2}$  and  $\mathbf{A}_j := \widehat{\Sigma}_{jj}^{-1/2}$ . Then  $\widehat{\mathbf{R}}_{ij} = \mathbf{A}_i \widehat{\Sigma}_{ij} \mathbf{A}_j$  and

$$\widehat{\mathbf{R}}_{ij} - \mathbf{R}_{ij} = \mathbf{A}_i (\widehat{\Sigma}_{ij} - \mathbf{R}_{ij}) \mathbf{A}_j + (\mathbf{A}_i \mathbf{R}_{ij} \mathbf{A}_j - \mathbf{R}_{ij}).$$

Using  $\|\mathbf{R}_{ij}\|_2 \leq 1$ , the triangle inequality, and Equation 39, on the event  $\varepsilon_{ij} \leq 1/2$  we obtain

$$\begin{aligned} \|\widehat{\mathbf{R}}_{ij} - \mathbf{R}_{ij}\|_2 &\leq \|\mathbf{A}_i\|_2 \|\widehat{\Sigma}_{ij} - \mathbf{R}_{ij}\|_2 \|\mathbf{A}_j\|_2 + \|(\mathbf{A}_i - \mathbf{I})\mathbf{R}_{ij}\mathbf{A}_j\|_2 + \|\mathbf{R}_{ij}(\mathbf{A}_j - \mathbf{I})\|_2 \\ &\leq (1 - \varepsilon_{ij})^{-1} \varepsilon_{ij} + \|\mathbf{A}_i - \mathbf{I}\|_2 \|\mathbf{A}_j\|_2 + \|\mathbf{A}_j - \mathbf{I}\|_2 \\ &\leq 2\varepsilon_{ij} + 2\varepsilon_{ij}\sqrt{2} + 2\varepsilon_{ij} \leq 7\varepsilon_{ij}. \end{aligned}$$

If  $\varepsilon_{ij} > 1/2$ , then the desired bound is trivial after enlarging constants, because both  $\|\widehat{\mathbf{R}}_{ij}\|_2 \leq 1$  and  $\|\mathbf{R}_{ij}\|_2 \leq 1$  (immediate from Cauchy–Schwarz on the empirical and population distributions), so  $\|\widehat{\mathbf{R}}_{ij} - \mathbf{R}_{ij}\|_2 \leq 2$ .

**Step 4: union bound over all pairs.** Set  $\delta_{ij} := \delta/N^2$  and take a union bound over all  $\binom{N}{2} \leq N^2/2$  pairs. Using  $2d + \log(4/\delta_{ij}) = 2d + \log(4N^2/\delta) \lesssim d + \log(N/\delta)$  and absorbing constants, we conclude that with probability at least  $1 - \delta$ , simultaneously for all  $1 \leq i < j \leq N$ ,

$$\|\widehat{\mathbf{R}}_{ij} - \mathbf{R}_{ij}\|_2 \leq C \kappa^2 \sqrt{\frac{d + \log(N/\delta)}{n}},$$

for a universal constant  $C > 0$ . This proves Equation 10.

**Step 5: subspace perturbation bound (Wedin).** Fix  $i < j$  and let  $\mathbf{E} := \widehat{\mathbf{R}}_{ij} - \mathbf{R}_{ij}$ . Let  $r := r_{ij}$  and let  $\mathcal{U}_{i|j}$  (resp.  $\widehat{\mathcal{U}}_{i|j}$ ) be the rank- $r$  left singular subspace of  $\mathbf{R}_{ij}$  (resp.  $\widehat{\mathbf{R}}_{ij}$ ). Let  $\Delta_{ij} := \sigma_r(\mathbf{R}_{ij}) - \sigma_{r+1}(\mathbf{R}_{ij}) > 0$ . By Weyl’s inequality, for all  $k$ ,  $|\sigma_k(\widehat{\mathbf{R}}_{ij}) - \sigma_k(\mathbf{R}_{ij})| \leq \|\mathbf{E}\|_2$ . Hence on the event  $\|\mathbf{E}\|_2 \leq \Delta_{ij}/2$ ,

$$\sigma_r(\widehat{\mathbf{R}}_{ij}) - \sigma_{r+1}(\widehat{\mathbf{R}}_{ij}) \geq (\sigma_r(\mathbf{R}_{ij}) - \|\mathbf{E}\|_2) - (\sigma_{r+1}(\mathbf{R}_{ij}) + \|\mathbf{E}\|_2) = \Delta_{ij} - 2\|\mathbf{E}\|_2 \geq \Delta_{ij}/2.$$

Wedin’s sin  $\Theta$  theorem for singular subspaces then gives

$$\|\sin \Theta(\widehat{\mathcal{U}}_{i|j}, \mathcal{U}_{i|j})\|_2 \leq \frac{\|\mathbf{E}\|_2}{\Delta_{ij}/2} = \frac{2\|\widehat{\mathbf{R}}_{ij} - \mathbf{R}_{ij}\|_2}{\Delta_{ij}},$$

which is Equation 11. Applying the same argument to  $\widehat{\mathbf{R}}_{ij}^\top$  and  $\mathbf{R}_{ij}^\top$  yields the identical bound for the right singular subspace  $\widehat{\mathcal{U}}_{j|i}$ .  $\square$

## 15 Additional Experimental Results

Methods	$\tilde{\mathbf{f}}_1$		$\tilde{\mathbf{f}}_2$		$\tilde{\mathbf{f}}_3$	
	$PA_{\text{mean}}$	$PA_{\text{max}}$	$PA_{\text{mean}}$	$PA_{\text{max}}$	$PA_{\text{mean}}$	$PA_{\text{max}}$
BarlowTwins	34.47 $\pm$ 0.20	86.87 $\pm$ 1.10	31.68 $\pm$ 0.16	82.34 $\pm$ 0.90	33.07 $\pm$ 0.29	84.62 $\pm$ 0.86
InfoNCE	5.12 $\pm$ 0.13	<b>6.93 <math>\pm</math> 0.46</b>	<b>4.40 <math>\pm</math> 0.12</b>	7.78 $\pm$ 0.24	5.92 $\pm$ 0.06	8.03 $\pm$ 0.33
W-MSE	<b>4.70 <math>\pm</math> 0.09</b>	7.50 $\pm$ 0.45	4.49 $\pm$ 0.02	<b>7.52 <math>\pm</math> 0.77</b>	5.02 $\pm$ 0.04	8.82 $\pm$ 0.32
GCCA	5.00 $\pm$ 0.15	6.98 $\pm$ 0.37	5.50 $\pm$ 0.10	8.03 $\pm$ 0.39	<b>3.87 <math>\pm</math> 0.01</b>	<b>7.72 <math>\pm</math> 0.62</b>

Table 4: Comparison of the mean and maximum principal angles ( $PA_{\text{mean}}$ ,  $PA_{\text{max}}$ ) on synthetic data ( $d_{S_i} = d_Z = 5, \forall i \in [3]$ ) under Poisson distribution ( $p_\phi$ ).

Methods	$\tilde{\mathbf{f}}_1$		$\tilde{\mathbf{f}}_2$		$\tilde{\mathbf{f}}_3$	
	$PA_{\text{mean}}$	$PA_{\text{max}}$	$PA_{\text{mean}}$	$PA_{\text{max}}$	$PA_{\text{mean}}$	$PA_{\text{max}}$
BarlowTwins	34.42 $\pm$ 0.19	86.24 $\pm$ 1.00	32.31 $\pm$ 0.30	79.76 $\pm$ 0.86	33.56 $\pm$ 0.42	84.23 $\pm$ 0.94
InfoNCE	3.98 $\pm$ 0.06	9.15 $\pm$ 0.66	5.49 $\pm$ 0.21	7.54 $\pm$ 0.28	<b>4.21 <math>\pm</math> 0.07</b>	<b>8.38 <math>\pm</math> 0.57</b>
W-MSE	4.13 $\pm$ 0.11	6.84 $\pm$ 0.34	<b>5.76 <math>\pm</math> 0.08</b>	<b>8.22 <math>\pm</math> 0.67</b>	5.00 $\pm$ 0.17	8.48 $\pm$ 0.49
GCCA	<b>4.89 <math>\pm</math> 0.14</b>	<b>8.00 <math>\pm</math> 0.42</b>	6.18 $\pm$ 0.31	8.26 $\pm$ 0.26	6.55 $\pm$ 0.09	8.17 $\pm$ 0.40

Table 5: Comparison of the mean and maximum principal angles ( $PA_{\text{mean}}$ ,  $PA_{\text{max}}$ ) on synthetic data ( $d_{S_i} = d_Z = 5, \forall i \in [3]$ ) under negative binomial distribution ( $p_\phi$ ).

Methods	$\tilde{\mathbf{f}}_1$		$\tilde{\mathbf{f}}_2$		$\tilde{\mathbf{f}}_3$	
	$PA_{\text{mean}}$	$PA_{\text{max}}$	$PA_{\text{mean}}$	$PA_{\text{max}}$	$PA_{\text{mean}}$	$PA_{\text{max}}$
BarlowTwins	33.81 $\pm$ 0.07	86.63 $\pm$ 0.95	32.88 $\pm$ 0.21	80.63 $\pm$ 0.66	33.83 $\pm$ 0.21	84.90 $\pm$ 0.85
InfoNCE	<b>3.54<math>\pm</math>0.15</b>	8.49 $\pm$ 0.54	5.59 $\pm$ 0.01	9.81 $\pm$ 0.35	5.13 $\pm$ 0.15	<b>6.05<math>\pm</math>0.64</b>
W-MSE	5.12 $\pm$ 0.01	8.05 $\pm$ 0.68	<b>4.74<math>\pm</math>0.01</b>	<b>7.83<math>\pm</math>0.62</b>	<b>4.59<math>\pm</math>0.01</b>	9.08 $\pm$ 0.52
GCCA	4.85 $\pm$ 0.04	<b>8.02<math>\pm</math>0.31</b>	4.97 $\pm$ 0.09	9.15 $\pm$ 0.30	5.58 $\pm$ 0.23	7.44 $\pm$ 0.53

Table 6: Comparison of the mean and maximum principal angles ( $PA_{\text{mean}}$ ,  $PA_{\text{max}}$ ) on synthetic data ( $d_{S_i} = d_Z = 5, \forall i \in [3]$ ) under Gamma distribution ( $p_\phi$ ).

Methods	$\tilde{\mathbf{f}}_1$		$\tilde{\mathbf{f}}_2$		$\tilde{\mathbf{f}}_3$	
	$PA_{\text{mean}}$	$PA_{\text{max}}$	$PA_{\text{mean}}$	$PA_{\text{max}}$	$PA_{\text{mean}}$	$PA_{\text{max}}$
BarlowTwins	34.05 $\pm$ 0.28	85.39 $\pm$ 0.88	31.78 $\pm$ 0.39	82.21 $\pm$ 0.80	33.94 $\pm$ 0.26	84.21 $\pm$ 0.83
InfoNCE	<b>4.20<math>\pm</math>0.05</b>	8.26 $\pm$ 0.34	5.87 $\pm$ 0.09	8.30 $\pm$ 0.35	6.00 $\pm$ 0.06	<b>7.85<math>\pm</math>0.54</b>
W-MSE	5.08 $\pm$ 0.16	8.37 $\pm$ 0.42	5.76 $\pm$ 0.04	<b>7.31<math>\pm</math>0.45</b>	5.07 $\pm$ 0.01	8.77 $\pm$ 0.47
GCCA	4.63 $\pm$ 0.01	<b>7.87<math>\pm</math>0.41</b>	<b>5.59<math>\pm</math>0.01</b>	9.45 $\pm$ 0.36	<b>4.08<math>\pm</math>0.22</b>	8.91 $\pm$ 0.60

Table 7: Comparison of the mean and maximum principal angles ( $PA_{\text{mean}}$ ,  $PA_{\text{max}}$ ) on synthetic data ( $d_{S_i} = d_Z = 5, \forall i \in [3]$ ) under Gaussian prior ( $p_\phi$ ).